

Measurement of hard double-parton interactions in $W(\rightarrow\ell) + 2$ -jet events at $\sqrt{s} = 7$ TeV with the ATLAS detector

This content has been downloaded from IOPscience. Please scroll down to see the full text.

2013 New J. Phys. 15 033038

(<http://iopscience.iop.org/1367-2630/15/3/033038>)

View [the table of contents for this issue](#), or go to the [journal homepage](#) for more

Download details:

IP Address: 159.149.193.149

This content was downloaded on 17/02/2017 at 11:42

Please note that [terms and conditions apply](#).

You may also be interested in:

[CMS Physics Technical Design Report, Volume II: Physics Performance](#)

The CMS Collaboration

[Precision measurements of the top quark mass from the Tevatron in the pre-LHC era](#)

Angela Barbaro Galtieri, Fabrizio Margaroli and Igor Volobouev

[Search for WH production with a light Higgs boson decaying to prompt electron-jets in proton–proton collisions at TeV with the ATLAS detector](#)

G Aad,
T Abajyan,
Wolfgang Wagner
B Abbott et al.

[Status of Higgs boson searches at the beginning of the LHC era](#)

A Sopczak

[Search for scalar leptoquarks in pp collisions at \$\sqrt{s} = 13\$ TeV with the ATLAS experiment](#)

The ATLAS Collaboration, M Aaboud, G Aad et al.

[Search for excited electrons and muons in TeV proton–proton collisions with the ATLAS detector](#)

G Aad, T Abajyan, B Abbott et al.

[Measurement of the cross-section of high transverse momentum vector bosons reconstructed as single jets and studies of jet substructure in pp collisions at \$\sqrt{s} = 7\$ TeV with the ATLAS detector](#)

G Aad, T Abajyan, B Abbott et al.

[Jet substructure at the Tevatron and LHC: new results, new tools, new benchmarks](#)

A Altheimer, S Arora, L Asquith et al.

Measurement of hard double-parton interactions in $W(\rightarrow \ell\nu) + 2$ -jet events at $\sqrt{s} = 7$ TeV with the ATLAS detector

The ATLAS Collaboration

New Journal of Physics **15** (2013) 033038 (39pp)

Received 29 January 2013

Published 25 March 2013

Online at <http://www.njp.org/>

doi:10.1088/1367-2630/15/3/033038

E-mail: atlas.publications@cern.ch

Abstract. The production of W bosons in association with two jets in proton–proton collisions at a centre-of-mass energy of $\sqrt{s} = 7$ TeV has been analysed for the presence of double-parton interactions using data corresponding to an integrated luminosity of 36 pb^{-1} , collected with the ATLAS detector at the Large Hadron Collider. The fraction of events arising from double-parton interactions, $f_{\text{DP}}^{(\text{D})}$, has been measured through the p_{T} balance between the two jets and amounts to $f_{\text{DP}}^{(\text{D})} = 0.08 \pm 0.01$ (stat.) ± 0.02 (sys.) for jets with transverse momentum $p_{\text{T}} > 20$ GeV and rapidity $|y| < 2.8$. This corresponds to a measurement of the effective area parameter for hard double-parton interactions of $\sigma_{\text{eff}} = 15 \pm 3$ (stat.) ${}_{-3}^{+5}$ (sys.) mb.

Contents

1. Introduction	2
2. Theoretical background	3
3. Strategy of the analysis	4
4. The ATLAS detector	6
5. Event selection	7
6. Monte Carlo (MC) simulation	8
6.1. Sample composition	8
6.2. Templates	9
7. Strategy validation	10
7.1. Double-parton interactions at detector level in the MC simulation	11
7.2. Influence of pile-up	11
7.3. Transition from detector level to parton level	12
7.4. Effect of p_T^{\max} value	13
7.5. Model dependence of Template A	14
8. Hadron-level studies	17
8.1. Determination of σ_{eff}	18
9. Conclusions	20
Acknowledgments	21
The ATLAS Collaboration	21
References	38

1. Introduction

Double-parton interactions (DPI) in hadron-initiated processes have been discussed in theoretical studies since the first days of the parton model [1–3]. These studies have subsequently been refined and reformulated in the framework of perturbative quantum chromodynamics for a variety of processes such as double Drell–Yan production, four-jet production, and W production associated with two jets [4–10]. Potential correlations in colour and spin space have been analysed theoretically [11], and evolution equations for multi-parton distribution functions have been derived [12]. The formalism [7, 8] to deal with DPI in hadronic interactions at a centre-of-mass energy \sqrt{s} may be summarized, assuming perturbative factorization, by

$$d\hat{\sigma}_{Y+Z}^{(\text{DPI})}(s) = \frac{m}{2\sigma_{\text{eff}}(s)} \int dx_{i_1} dx_{j_1} dx_{i_2} dx_{j_2} [f_{i_1 j_1}(x_{i_1}, x_{j_1}, \mu_F) \times f_{i_2 j_2}(x_{i_2}, x_{j_2}, \mu_F) d\hat{\sigma}_{i_1 i_2 \rightarrow Y}(x_{i_1}, x_{i_2}, s) d\hat{\sigma}_{j_1 j_2 \rightarrow Z}(x_{j_1}, x_{j_2}, s)], \quad (1)$$

where $d\hat{\sigma}_{Y+Z}^{(\text{DPI})}$ is the differential double-parton interaction cross section for the inclusive production of a combined system $Y + Z$ at a given \sqrt{s} , and the $d\hat{\sigma}_{k_1 k_2 \rightarrow Y(Z)}$ is the differential partonic cross section for the production of a system Y or Z in the collision of partons k_1 and k_2 . The symmetry factor m is equal to one if $Y = Z$ and equal to two if $Y \neq Z$. The $f_{ij}(x_i, x_j, \mu_F)$ are the double-parton distribution functions (DPDFs) evaluated at a specific factorization scale, μ_F . The integration over the momentum fractions x_i and x_j of the two partons from the

same proton is constrained by energy conservation such that $x_i + x_j \leq 1$. A summation over all possible parton combinations is implicitly assumed. Typically, the DPDFs are expressed in terms of the conventional single parton distributions using a factorized *ansatz* [7, 8], namely

$$f_{ij}(x_i, x_j, \mu_F) = f_i(x_i, \mu_F) f_j(x_j, \mu_F) (1 - x_i - x_j) \Theta(1 - x_i - x_j), \quad (2)$$

where the factor $(1 - x_i - x_j)\Theta(1 - x_i - x_j)$ implements the kinematic constraint and $\Theta(x)$ is the Heaviside step function. The effective area parameter for DPI, $\sigma_{\text{eff}}(s)$, is defined at the parton level and, in the formalism outlined here, is independent of the process and of the phase-space under consideration. Naively, it can be related to the geometrical size of the proton, leading to an estimate of $\sigma_{\text{eff}} \approx \pi R_p^2 \approx 50$ mb, where R_p is the proton radius. Alternatively, σ_{eff} can be connected to the inelastic cross section, which would lead to $\sigma_{\text{eff}} \approx \sigma_{\text{inel}} \approx 70$ mb at $\sqrt{s} = 7$ TeV [13, 14].

A number of measurements of $\sigma_{\text{eff}}(s)$ have been performed in pp or $p\bar{p}$ collisions at centre-of-mass energies of 63 GeV [15], 630 GeV [16], 1.8 TeV [17, 18] and 1.96 TeV [19]. The measured values range from about 5 mb at the lowest energy to about 15 mb at Tevatron energies. Attempts to understand these values have used non-trivial correlations between the two scattering systems to explain the differences between these measured values [20, 21].

In the scientific programme of the Large Hadron Collider (LHC), issues related to multi-parton interactions have attracted increasing attention [22–35]. This surge of interest is due to the higher centre-of-mass energy leading to enhanced parton densities and therefore to an anticipated larger impact of such effects on a multitude of physics signatures. The high energy and high luminosity available at the LHC also implies that multiple interactions should occur at higher transverse momentum, p_T , offering the possibility to further study these interactions in a variety of processes. This paper presents a measurement of σ_{eff} in pp collisions at $\sqrt{s} = 7$ TeV performed with the ATLAS detector [36], using events with two jets produced in association with a W boson.

2. Theoretical background

The quantity σ_{eff} parameterizes the double-parton interaction part of the production cross section for a composite system ($Y + Z$) in hadronic collisions. Assuming no correlations between the two systems, the differential cross section $\hat{\sigma}_{Y+Z}^{(\text{tot})}$ for the production of $Y + Z$ consists of a direct part, $\hat{\sigma}_{Y+Z}^{(\text{SPI})}$, originating from single-parton interaction, and a double-parton interaction contribution, $\hat{\sigma}_{Y+Z}^{(\text{DPI})}$,

$$d\hat{\sigma}_{Y+Z}^{(\text{tot})}(s) = d\hat{\sigma}_{Y+Z}^{(\text{SPI})}(s) + d\hat{\sigma}_{Y+Z}^{(\text{DPI})}(s) = d\hat{\sigma}_{Y+Z}^{(\text{SPI})}(s) + \frac{d\hat{\sigma}_Y(s) \cdot d\hat{\sigma}_Z(s)}{\sigma_{\text{eff}}(s)}, \quad (3)$$

where $d\hat{\sigma}_Y(s)$ and $d\hat{\sigma}_Z(s)$ correspond to the differential cross sections of processes Y and Z respectively and the symmetry factor m from equation (1) has been set equal to two.

After integrating the differential cross sections in equation (3) over the phase space defined by the selection cuts on the Y and Z systems as appropriate for the analysis and solving the equation for σ_{eff} ,

$$\sigma_{\text{eff}}(s) = \frac{\hat{\sigma}_Y(s) \cdot \hat{\sigma}_Z(s)}{\hat{\sigma}_{Y+Z}^{(\text{DPI})}(s)} = \frac{\hat{\sigma}_Y(s) \cdot \hat{\sigma}_Z(s)}{\hat{\sigma}_{Y+Z}^{(\text{tot})}(s) - \hat{\sigma}_{Y+Z}^{(\text{SPI})}(s)}. \quad (4)$$

With the exception of the direct component, $\hat{\sigma}_{Y+Z}^{(\text{SPI})}(s)$, for which theoretical input (for example in the form of a Monte Carlo (MC) event generator) needs to be employed, all quantities in

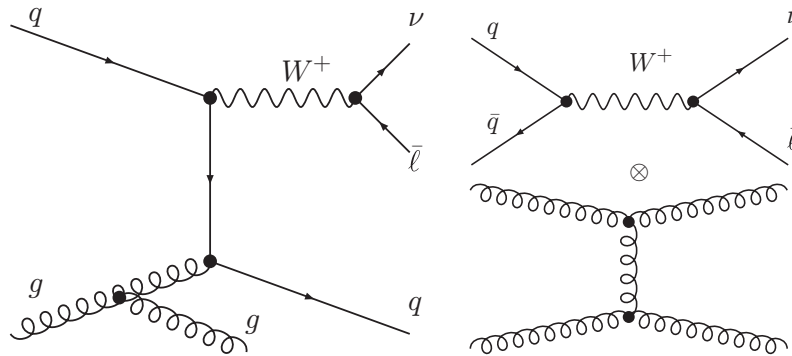


Figure 1. Examples of leading-order Feynman diagrams for the direct (left) and double-parton interaction (right) components in the production of a W^+ +2-jet system. These contributions are defined in equation (3) with the identification $Y \rightarrow W^+$ and $Z \rightarrow 2$ jets.

equation (4) may be directly taken from data, provided that the simple factorization picture is applicable. This assumes that the proposed correlation in the DPDFs, the factor $(1 - x_i - x_j)$ present in equation (2), is close to 1. There will be other effects which will eventually lead to a breakdown of this simple picture in some corners of phase space; for example total energy conservation, flavour conservation rules, or, more intricately, complicated interactions between the initial- or final-state partons [24, 37–40] which potentially correlate the two systems in a non-trivial way. However, for certain processes and selection cuts, such effects may turn out to be negligible. In the following, when referring to data and integrating over the hadronic final states, $\hat{\sigma}(s)$ will be replaced by $\sigma(s)$.

For the case of $W + 2$ -jet production discussed in this paper, the cross sections at leading order are related to Feynman diagrams such as those depicted in figure 1. In general, calculations of the differential cross sections for the production of any system Y are inclusive. In particular, in the calculation of the leading-order W cross section, the production of additional jets is implicitly included. These extra jets may populate a phase space constrained from below by the factorization scale μ_F . In this study, in which jets are defined by a transverse momentum requirement of $p_T > 20$ GeV, this implies that the cross sections entering the calculation of σ_{eff} correspond to the production of a W boson with no accompanying jets, of a W boson accompanied by exactly two jets and a hadronic final state consisting of exclusive two jets.

3. Strategy of the analysis

The cornerstone of the analysis is the extraction of the fraction of $W + 2$ -jet events produced in pp interactions in which the jets originate from a hard DPI. This fraction is subsequently used to determine the value of σ_{eff} . The sample of $W + 2$ -jet candidate events is selected from data recorded by the ATLAS detector with the W boson identified through its leptonic decays into $e\nu$ and $\mu\nu$. The fraction $f_{\text{DP}}^{(\text{D})}$, where the superscript D refers to detector level, of $W + 2$ -jet events originating from DPI is defined by

$$f_{\text{DP}}^{(\text{D})} = \frac{N_{W_{0j}+2j_{\text{DPI}}}}{N_{W+2j}} = \frac{N_{W_{0j}+2j_{\text{DPI}}}}{N_{W_{2j}} + N_{W_{0j}+2j_{\text{DPI}}}}, \quad (5)$$

where N_{W+2j} is the total number of $W + 2$ -jet events, $N_{W_{2j}}$ is the number of events in which the production of the two jets is directly associated with the production of the W boson (single-parton interaction), and $N_{W_{0j}+2j_{\text{DPI}}}$ is the number of events in which the production of the two jets originates from DPI. In order to extract $f_{\text{DP}}^{(\text{D})}$, a minimization fit to the distribution of an observable is performed. The observable is chosen such that it shows good discriminating power between the direct production of a W boson with two jets (W_{2j}) and the production of a W boson in association with zero jets in addition to another parton-parton scatter resulting in two jets ($W_{0j} + 2j_{\text{DPI}}$). The fit is performed to the normalized, detector-level, background-corrected data distribution of the observable using two normalized templates, denoted by A and B .

Template A represents the expected contribution to the distribution of the chosen observable from W_{2j} events, and Template B that from $W_{0j} + 2j_{\text{DPI}}$ events. The fit function is given by $(1 - f_{\text{DP}}^{(\text{D})}) \cdot A + f_{\text{DP}}^{(\text{D})} \cdot B$. The details of how the templates are constructed and how the fit is performed, together with supporting MC studies, are described in section 6. The relevant part of the equation defining σ_{eff} , equation (4), reads

$$\sigma_{\text{eff}} = \frac{\sigma_{W_{0j}} \cdot \sigma_{2j}}{\sigma_{W_{0j}+2j_{\text{DPI}}}}. \quad (6)$$

Here, $\sigma_{W_{0j}}$, $\sigma_{W_{0j}+2j_{\text{DPI}}}$ and σ_{2j} are the production cross sections of W_{0j} , $W_{0j} + 2j_{\text{DPI}}$ and exclusive dijet ($2j$) events, respectively. These cross sections are related to the respective number of events N through the relation

$$\sigma = \frac{N}{A C \varepsilon \mathcal{L}}, \quad (7)$$

where C denotes the corrections for unfolding to the particle level including reconstruction effects, A is the geometrical acceptance, ε is the trigger efficiency, and \mathcal{L} is the integrated luminosity. The assumption of factorization between the W boson and the $2j$ system leads to some simplifications. Firstly, the kinematics of the W boson does not influence the kinematic distributions of the DPI system, either at the detector level or at the hadron level, once corrections involving the impact of jets on W reconstruction and vice versa have been made. Secondly, the kinematics of the jets originating from DPI may be modelled by the kinematics of single-scatter dijet events. Therefore

$$\mathcal{A}_{W_{0j}+2j_{\text{DPI}}} \cdot C_{W_{0j}+2j_{\text{DPI}}} = \mathcal{A}_{W_{0j}} \cdot C_{W_{0j}} \cdot \mathcal{A}_{2j} \cdot C_{2j}. \quad (8)$$

Finally, the $W_{0j} + 2j_{\text{DPI}}$ and W_{0j} events are collected using the same trigger selection. Taken together, this results in luminosity and efficiency cancellations and σ_{eff} is given by

$$\sigma_{\text{eff}} = \frac{N_{W_{0j}} N_{2j}}{f_{\text{DP}}^{(\text{D})} \cdot N_{W+2j}} \cdot \frac{1}{\varepsilon_{2j}} \cdot \frac{1}{\mathcal{L}_{2j}}. \quad (9)$$

In a previous phenomenological study [10] it was suggested to use the transverse momentum of the W boson, p_{T}^W , as the key observable to distinguish double-parton scattering production of $W + 2$ -jet events from the direct production channel. This observable suffers from experimental inaccuracies due to the fact that the kinematics of the W boson must be reconstructed from the missing transverse momentum, $E_{\text{T}}^{\text{miss}}$. Alternatively, one could try to use the p_{T} distribution of the individual jets, but their discrimination power is limited by uncertainties stemming from the jet energy scale. This leaves correlations between the jets or between the jets and the kinematics of the W as further possibilities, one being the azimuthal correlation of the two leading jets in the transverse plane. In the picture of DPI production

advocated here, the kinematics of the W boson and the dijet systems are decorrelated. Therefore, the momenta of the two jets must compensate each other in the transverse plane, orienting them back-to-back in azimuthal angle, rendering, in principle, this angular separation between the jets a useful observable. However, due to the distortion of this variable by various systematic effects, in particular multiple proton–proton interactions (pile-up) and the underlying event, in this analysis the balance in transverse momenta of the two jets is used instead, quantified by

$$\Delta_{\text{jets}} = |\vec{p}_{\text{T}}^{J_1} + \vec{p}_{\text{T}}^{J_2}|, \quad (10)$$

where $\vec{p}_{\text{T}}^{J_1}$ and $\vec{p}_{\text{T}}^{J_2}$ are the transverse momentum vectors of the two leading jets. Anticipating a potentially large dependence of Δ_{jets} on the jet energy scale, another observable, the transverse momentum of the dijet system normalized by the sum of the individual transverse momenta, $\Delta_{\text{jets}}^{\text{n}}$, is constructed,

$$\Delta_{\text{jets}}^{\text{n}} = \frac{|\vec{p}_{\text{T}}^{J_1} + \vec{p}_{\text{T}}^{J_2}|}{|\vec{p}_{\text{T}}^{J_1}| + |\vec{p}_{\text{T}}^{J_2}|}. \quad (11)$$

The distribution of $\Delta_{\text{jets}}^{\text{n}}$ is employed to drive the fit from which $f_{\text{DP}}^{(\text{D})}$ is obtained, while the distribution of Δ_{jets} allows further checks.

4. The ATLAS detector

The ATLAS detector [36] comprises a superconducting solenoid surrounding the inner detector (ID), as well as electromagnetic and hadronic calorimeters and a large superconducting toroid magnet system instrumented with muon-detection chambers. The ID system is immersed in a 2 T axial magnetic field and provides tracking information for charged particles in a pseudorapidity range matched by the precise measurements of the electromagnetic calorimeter. The silicon pixel and microstrip tracking detectors cover the pseudorapidity¹ range $|\eta| < 2.5$. The transition radiation tracker, which surrounds the silicon detectors, can perform tracking up to $|\eta| = 2.0$ and contributes to electron identification. The liquid-argon electromagnetic calorimeter is divided into one barrel ($|\eta| < 1.475$) and two end-cap components ($1.375 < |\eta| < 3.2$). It uses an accordion geometry to ensure fast and uniform response, and fine segmentation for optimum reconstruction and identification of electrons and photons. The iron/scintillator tile hadronic calorimeter consists of a barrel covering the region $|\eta| < 1.0$, and two extended barrels in the range $0.8 < |\eta| < 1.7$. The muon spectrometer is based on three large superconducting toroids with coils arranged in an eight-fold symmetry around the calorimeters, covering a range of $|\eta| < 2.7$. Over most of this range, precision measurements of the track coordinates in the principal bending direction of the magnetic field are provided by monitored drift tubes. At large pseudorapidities ($2.0 < |\eta| < 2.7$), cathode strip chambers with higher granularity are used in the innermost station. The ATLAS detector has a three-level trigger system consisting of level-1, level-2 and the event filter (L1, L2 and EF). The L1 trigger rate at design luminosity is approximately 75 kHz. The L2 and EF triggers reduced the recorded event rate in 2010 to approximately 200 Hz.

¹ ATLAS uses a right-handed coordinate system with its origin at the nominal interaction point (IP) in the centre of the detector and the z -axis along the beam pipe. The x -axis points from the IP to the centre of the LHC ring, and the y -axis points upward. Cylindrical coordinates (r, ϕ) are used in the transverse plane, ϕ being the azimuthal angle around the beam pipe. The pseudorapidity is defined in terms of the polar angle θ as $\eta = -\ln \tan(\theta/2)$. The rapidity of a particle with respect to the beam axis is defined as $y = \frac{1}{2} \ln \frac{E+p_z}{E-p_z}$.

5. Event selection

The dataset collected in 2010, corresponding to approximately 36 pb^{-1} of integrated luminosity, is used in this analysis. The rate of overlapping uncorrelated proton–proton interactions occurring within the same bunch crossing (also referred to as pile-up) gradually increased up an average of about two interactions per bunch-crossing throughout the data-taking period. The selection of W events is based on the leptonic $W \rightarrow e\nu$ and $W \rightarrow \mu\nu$ decay channels and follows the one already described in [41], where more details can be found. It differs in the requirements on the jet transverse momentum and rapidity. The objects required for the different samples and templates needed in the analysis were selected as described in the following.

To select electron candidates, clusters formed from energy depositions in the electromagnetic calorimeter are required with matched tracks in the ID, with the further requirement that the cluster shapes are consistent with electromagnetic showers initiated by electrons. Such electron candidates were required to have transverse momenta $p_{\text{T}}^{\ell} > 20 \text{ GeV}$ and $|\eta| < 2.47$. Electrons reconstructed in the transition region between the barrel and end-cap calorimeters ($1.37 < |\eta| < 1.52$) or falling into inactive regions of the calorimeter were excluded. The standard isolation requirement on electron candidates [42] was applied to improve multi-jet background rejection.

Muon candidates were selected by requiring $p_{\text{T}}^{\ell} > 20 \text{ GeV}$ and $|\eta| < 2.4$. They were reconstructed requiring both the muon spectrometer and the ID information. Additional requirements were applied to the number of hits used to reconstruct the track in the ID. Furthermore, the z -coordinate of the muon longitudinal impact parameter with respect to the interaction vertex was required to be less than 10 mm. A selection requirement was applied to the significance of the track transverse impact parameter to ensure that the muon was prompt. The standard isolation requirements were applied to the muons [43] to improve multi-jet background rejection.

To select events with a W boson, in addition to requiring exactly one lepton (e or μ) in the event, requirements were imposed on $E_{\text{T}}^{\text{miss}}$ and the transverse mass, m_{T} . The $E_{\text{T}}^{\text{miss}}$ was calculated using the reconstructed physics objects, the remaining energy deposits in the calorimeter, and the ID tracking information. The m_{T} is defined in terms of the missing transverse energy and the charged lepton transverse momentum as $m_{\text{T}} = [2p_{\text{T}}^{\ell}E_{\text{T}}^{\text{miss}}(1 - \cos\Delta\phi_{\ell, E_{\text{T}}^{\text{miss}}})]^{1/2}$, where $\Delta\phi_{\ell, E_{\text{T}}^{\text{miss}}}$ is the angle between the lepton transverse momentum and the missing transverse momentum. Events were required to have $E_{\text{T}}^{\text{miss}} > 25 \text{ GeV}$ and $m_{\text{T}} > 40 \text{ GeV}$.

Jets are defined using the anti- k_t algorithm [44] with radius parameter $R = 0.4$. The jets were reconstructed from clusters built from calorimeter cells, initially not accounting for different calorimeter response to electrons and hadrons, and subsequently calibrated [45]. Jets were required to have $p_{\text{T}} > 20 \text{ GeV}$ and $|y| < 2.8$. All jets within $\Delta R = \sqrt{(\Delta\eta)^2 + (\Delta\phi)^2} = 0.5$ of a selected electron or muon were removed from the analysis. The number of jets originating from pile-up interactions was reduced by applying a selection requirement on the jet-vertex fraction (JVF), which is defined for each jet in an event. After associating tracks to jets with a matching in $\Delta R(\text{track}, \text{jet})$, requiring $\Delta R < 0.5$, the JVF was computed for each jet as the scalar sum of the transverse momenta of all matched tracks from the interaction vertex divided by the total jet-matched track transverse momentum from all vertices. Jets were removed from the analysis if $\text{JVF} < 0.75$. This selection was not applied to jets that lie outside the acceptance of the ID or to those jets without matching tracks.

With these selections, the following samples have been constructed:

- $W + 0$ -jet sample, consisting of events passing either the $W \rightarrow e\nu$ or $W \rightarrow \mu\nu$ selection and where no jets are found in addition to the W decay products;
- $W + 2$ -jet sample, consisting of events passing either the $W \rightarrow e\nu$ or $W \rightarrow \mu\nu$ selection and where exactly two jets are found in addition to the W decay products;
- dijet sample, which consists of events recorded with exactly two jets. The selected events were taken using the Minimum Bias Trigger Scintillators and Zero Degree Calorimeters, which have been shown [46] to be unbiased and fully efficient for jet-based measurements. A subset of this sample with negligible pile-up, corresponding to the first $184 \mu\text{b}^{-1}$ of data taking, was used to calculate the N_{2j} term described in equation (9).

6. Monte Carlo (MC) simulation

The treatment of MC simulation and background estimation is based on that described in [41]. The MC samples of events in this analysis were produced with CTEQ6L1 [49] parton distribution functions. The simulation of detector effects was performed with GEANT4 [47]. These simulated event samples [48] were used for the background and signal estimates. They were reweighted such that they matched the data in the number of reconstructed vertices per event.

To simulate the W boson signal, samples of events were generated using ALPGEN [50] with the MLM [51] matching scheme, interfaced with HERWIG [52] v6.510 and JIMMY [53] v4.31 (AUET2 tune), together referred to as A+H+J samples. SHERPA [54] v1.3.1, with the CKKW [55] merging, and with the default underlying event tune, was also used to simulate W events.

MC generators populate the activity in a hard-scattering event with additional parton-parton scatters, the average number of which depends on the assumed lowest- p_T threshold of additional soft partons and the available phase space. The extra scatters are commonly called multi-parton interactions (MPI). Some of the scattered partons will materialize as jets of hadrons above a certain p_T threshold. Others will result in extra hadronic activity added to the original hard scattering in the event. In this analysis, a threshold on the p_T of the scattered parton, p_T^{max} , is introduced, whose purpose is to separate these two classes of hard and soft scatters.

In the A+H+J simulation, a sample of events without DPI may be obtained by removing events with two or more additional $2 \rightarrow 2$ parton scatters with a parton-level p_T above a preset p_T^{max} . In SHERPA, the MIHANDLER switch is used to switch off the effects of DPI.

As for potential sources of physics background to the W signal, PYTHIA6 [56] was used to produce MC samples for the modelling of multi-jet and $Z \rightarrow \ell\ell$ physics contributions. POWHEG [57] was used to model the $t\bar{t}$ background contribution. MC@NLO [58] was used to provide MC samples for the modelling of single top quark and diboson contributions.

6.1. Sample composition

The contributions of electroweak backgrounds ($Z \rightarrow \ell\ell$ and diboson production), as well as $W \rightarrow \tau\nu$, $t\bar{t}$ and single top quark production to both channels are estimated using MC simulation. The absolute normalization is derived using the total theoretical cross sections and

corrected using the acceptance and efficiency losses of the event selection. These backgrounds amount to about 5% of the selected events in the electron channel (dominated by the $W \rightarrow \tau\nu$ contribution), and about 8% in the muon channel (dominated by the $Z \rightarrow \ell\ell$ contribution). The contributions from non-physics backgrounds were considered to be negligible. The background contributions to the selected events can also come from multi-jet production processes in which a lepton is either produced through the decay of a hadron containing a heavy quark, the decay-in-flight of a light meson to a muon, or through a coincidence of hadronic signatures mimicking the characteristics of a lepton. The shape and normalization of the distribution of various observables in multi-jet backgrounds are determined using data-driven methods in both analysis channels. For the $W \rightarrow e\nu$ selection, the background shape is obtained by reversing certain requirements on shower shape in the calorimeter in the data selection procedure to produce a multi-jet enriched sample. Similarly, to estimate the multi-jet contribution to $W \rightarrow \mu\nu$, the background shape is obtained from data by inverting the requirements on the muon impact parameter and its significance to produce a multi-jet enriched sample. These multi-jet-enriched samples give the shapes of the distributions of multi-jet background observables. Their normalization in the selected data sample is determined by fitting a linear combination of the multi-jet E_T^{miss} shape, and that for the leptonic contribution, to the observed E_T^{miss} distribution. The multi-jet background was thus estimated to contribute about 14% of the selected events in the electron channel and 6% in the muon channel in the selected $W+2$ -jet sample.

Figure 2 shows the distributions of the two key observables Δ_{jets}^n and Δ_{jets} obtained in selected $W+2$ -jet events. The data are compared with the results from the SHERPA and A + H + J MC samples with their default MPI treatment, after adding the background contributions, which are also shown in the plots.

6.2. Templates

The fit, from which $f_{\text{DP}}^{(\text{D})}$ is extracted, is performed by comparing the distribution of Δ_{jets}^n at detector level in background-corrected data with two templates.

- **Template A ‘DPI-off’**—normalized distribution of the discriminating variable for a sample in which the two jets originate from a primary scatter. The main sample for Template A was produced by A + H + J. To construct Template A, it is necessary to remove hard MPI candidate events from the generated sample. Relevant events contain the W boson as well as at least two outgoing partons, i.e., partons that stem from the hardest scatter, or that originate from a secondary scatter. Events containing two or more secondary partons above a defined cutoff scale, $p_T^{\text{max}} = 15$ GeV, are classified as DPI events and therefore rejected. The value of p_T^{max} and its impact on the analysis are further discussed in section 7.4. An alternative modelling of Template A was obtained using the SHERPA MC sample where MPI has been switched off altogether. This removes all secondary perturbative parton scatters, which effectively produce transverse momenta in the range $p_T > 3.5$ GeV, but it retains the initial-state radiation off the incoming legs of the hard matrix element, the generation of intrinsic transverse momentum and the fragmentation of beam remnants. As an example, the distributions of Δ_{jets}^n and Δ_{jets} for simulated $W+2$ -jet events are displayed in figure 3. These distributions were obtained from A + H + J, both inclusively and with DPI switched off (i.e. Template A). The distributions show sensitivity to the effect of double-parton scattering, especially at low values of Δ_{jets}^n and Δ_{jets} .

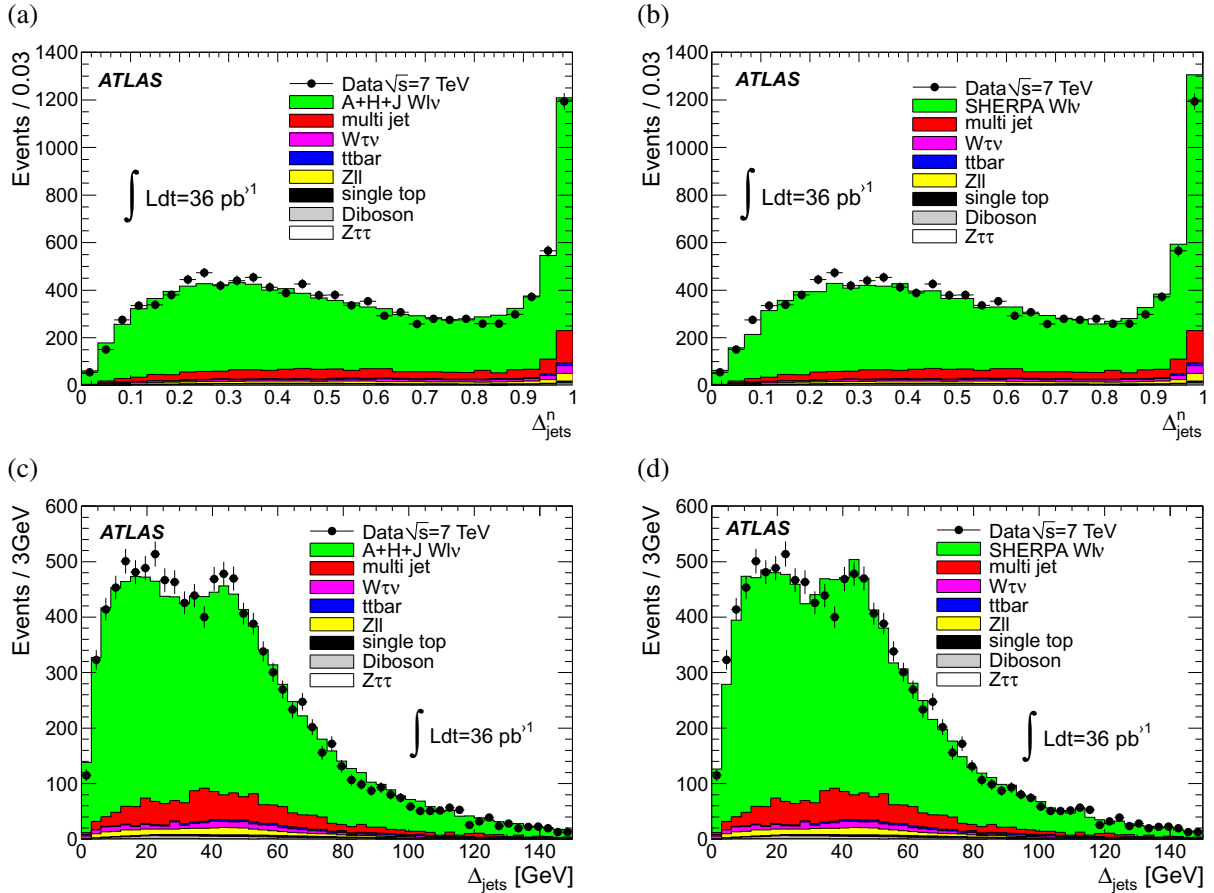


Figure 2. The (a), (b) Δ_{jets}^n and (c), (d) Δ_{jets} distributions at detector level for events passing the $W+2$ -jet selection cuts. The distributions from data (dots) are compared with (a), (c) $A+H+J$ and (b), (d) SHERPA signal MC (histogram) predictions. In addition, physics backgrounds, also shown, have been added in due proportion to the MC histogram.

- Template B ‘DPI-only’—normalized distribution of the discriminating variable for a sample in which both jets originate from a DPI scatter. The dijet sample described in section 5 was used to approximate the DPI template. The fractional difference between the final results when using the dijet PYTHIA6 MC as Template B in place of dijet data was found to be well below the per cent level.

7. Strategy validation

For the purpose of validation studies, the inclusive $A+H+J$ sample was employed to mimic the data and its distribution was fitted as a combination of Templates A and B . As for the fits to the data distributions, Template A is based on the $A+H+J$ sample with $p_T^{\text{max}} = 15$ GeV and Template B is based on the dijet data sample. The fitted value for $f_{\text{DP}}^{(\text{MC})}$ thus obtained, once corrected for pile-up effects, can be compared to the expected fraction of DPI directly extracted at the parton level from the event record of the $A+H+J$ sample.

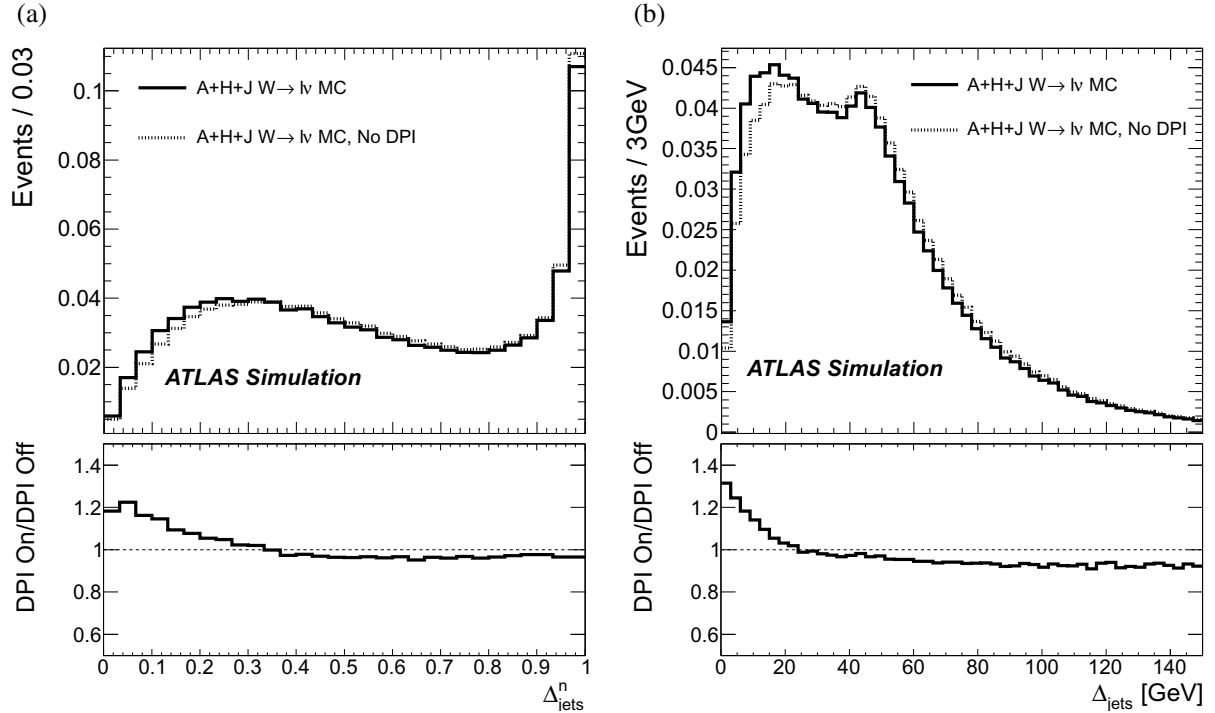


Figure 3. Comparison of the shapes of (a) Δ_{jets}^n and (b) Δ_{jets} distributions, at detector level, for selected $W \rightarrow \ell\nu + 2\text{-jet}$ events as expected in A + H + J, with DPI on and off (Template A). The lower panels show the respective ratios of the DPI-on and DPI-off expectations.

7.1. Double-parton interactions at detector level in the MC simulation

The fit of the combination of Templates A and B to the nominal A + H + J Δ_{jets}^n distribution yields

$$f_{\text{DP}}^{(\text{MC})}(\Delta_{\text{jets}}^n) = 0.051 \pm 0.003 \quad (\text{stat.}). \quad (12)$$

In the fit to the distribution of Δ_{jets}^n , events with $\Delta_{\text{jets}}^n > 0.93$ (corresponding to the last two bins of the fit) were ignored, since they represent configurations with two nearly parallel jets and therefore rather test the parton shower model. The fit minimization, when performed to the Δ_{jets} instead of the Δ_{jets}^n distribution, resulted in a value $f_{\text{DP}}^{(\text{MC})}(\Delta_{\text{jets}})$ that was within 13% of $f_{\text{DP}}^{(\text{MC})}(\Delta_{\text{jets}}^n)$. The resulting description of the distributions in Δ_{jets}^n and Δ_{jets} by the combination of the Templates A and B, using $f_{\text{DP}}^{(\text{MC})}(\Delta_{\text{jets}}^n)$, are shown in figure 4.

7.2. Influence of pile-up

In order to account for the influence of pile-up, the extraction of $f_{\text{DP}}^{(\text{MC})}$ was repeated after selecting only events with the requirement of exactly one reconstructed vertex, imposed on both the inclusive A + H + J sample and Template A. A subset of dijet events from earlier data-taking periods, where the effects of pile-up were smaller, was used to model Template B. In this way, the fitted value of $f_{\text{DP}}^{(\text{MC})}$ represents the DPI rate that would be extracted in the absence of

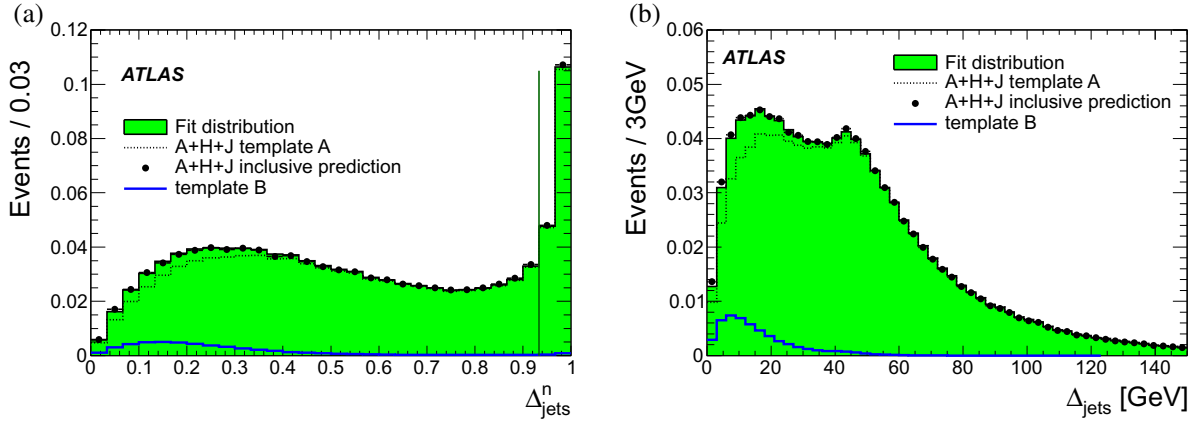


Figure 4. Distribution of (a) Δ_{jets}^n and (b) Δ_{jets} in the inclusive A + H + J pseudo-data (dots) compared to the results of fitting Δ_{jets}^n by a linear combination of Template A (dashed line) extracted from this sample and of Template B obtained from the dijet data (blue solid line). The result is shown as the green histogram. The bins to the right of the vertical dash-dotted line were excluded from the fit. The pseudo-data and the overall fit have been normalized to unity, Template A to $1 - f_{\text{DP}}^{(\text{MC})}(\Delta_{\text{jets}}^n)$ and Template B to $f_{\text{DP}}^{(\text{MC})}(\Delta_{\text{jets}}^n)$.

pile-up. The result is

$$f_{\text{DP}}^{(\text{MC})}(\Delta_{\text{jets}}^n) = 0.059 \pm 0.007 \quad (\text{stat.}), \quad (13)$$

which is in good agreement with that obtained from a fit to the Δ_{jets} distribution. The ratio, $r_{\text{pile-up}}$, of the $f_{\text{DP}}^{(\text{MC})}$ value with the one-vertex requirement to that without the requirement, without accounting for the effect of correlations², is $r_{\text{pile-up}} = 1.17 \pm 0.15(\text{stat.})$. A direct extraction of $f_{\text{DP}}^{(\text{D})}$ using only single pp interactions is not possible due to the small numbers of events in the data. For this reason, the ratio is used to correct $f_{\text{DP}}^{(\text{D})}$ to the result that would have been obtained in the case of single interactions. The statistical uncertainty on $r_{\text{pile-up}}$ is duly propagated as a systematic uncertainty whenever appropriate.

7.3. Transition from detector level to parton level

An important question, central to this analysis, is whether the σ_{eff} extracted at detector level can be related to the same quantity at the parton level. This is relevant because the value of σ_{eff} used in theoretical applications is typically defined at parton level only. This question can be translated into how close the DPI rate at parton level, $f_{\text{DP}}^{(\text{P})}$, is to the extracted DPI rate at detector level in the MC samples, $f_{\text{DP}}^{(\text{MC})}$. The parton-level DPI fraction is defined as

$$f_{\text{DP}}^{(\text{P})} = \frac{N^{\text{P}}(W_{0\text{j}} + 2j_{\text{DPi}})}{N^{\text{P}}(W_{0\text{j}} + 2j_{\text{DPi}}) + N^{\text{P}}(W_{2\text{j}})}, \quad (14)$$

² The impact of including the correlations is estimated to result in a maximum reduction of the statistical uncertainty on $r_{\text{pile-up}}$ to 0.12.

where the various N^P are the number of corresponding events at parton level. Here, the jets are directly identified with outgoing partons, with a fiducial acceptance chosen such that it matches that of the jets at detector level,

$$p_T^P \geq 20 \text{ GeV}, \quad |y^P| \leq 2.8 \quad \text{and} \quad \Delta R_{P\ell} > 0.5, \quad (15)$$

where ℓ denotes charged leptons and P the partons, as recorded at the generator level. The parton-level counting of the quantities $N^P(W_{0j} + 2j_{\text{DPI}})$ and $N^P(W_{2j})$ was performed in the inclusive A + H + J MC sample after selection of W+2-jet events, and yielded

$$f_{\text{DP}}^{(P)}(\Delta_{\text{jets}}^n) = 0.064 \pm 0.001 \quad (\text{stat.}), \quad (16)$$

which is within 10% of the equivalent quantity at detector level, $f_{\text{DP}}^{(\text{MC})}$.

7.4. Effect of p_T^{max} value

There could be sizable differences between the DPI-off samples provided by A + H + J and SHERPA. The origin of these differences has been identified as the difference in the extent to which softer MPI, at scales below the dijet transverse momenta, are included in the samples. In SHERPA, the only option is to switch off all such secondary interactions, while in A + H + J this can be steered through the p_T^{max} cut. In the A + H + J samples, events are removed from the inclusive sample if the p_T in secondary parton-parton scatters is above $p_T^{\text{max}} = 15 \text{ GeV}$. All softer MPI scatters are left in the sample. In contrast, in the DPI-off SHERPA sample, *all* secondary parton scatters are switched off, corresponding roughly to a $p_T^{\text{max}} \approx 3.5 \text{ GeV}$. To see how closely the two models can agree, p_T^{max} in A + H + J was reduced to 3.5 GeV. Despite intrinsic differences in the MPI modelling, this choice replicates the SHERPA results to within 10%, as is discussed in section 7.5.1.

In this particular analysis, it is desirable to include these soft MPI partons in both templates. In Template B they are present by default, and in Template A they must also be allowed as they do form a contribution to the direct production of W + 2-jet events in nature, which Template A is set up to model. However, there is also an upper constraint on this threshold, since $W_{0j} + 2j_{\text{DPI}}$ events where the jets have p_T above 20 GeV should not enter Template A. To determine the optimal p_T^{max} , alternative predictions for Template A with different p_T^{max} values were constructed from the inclusive A + H + J sample. Fits to Δ_{jets}^n distributions with different values of p_T^{max} in the A + H + J sample forming Template A were obtained. At low p_T^{max} values, $\leq 7.5 \text{ GeV}$, the fits do not show good agreement with the A + H + J distribution, since then partons from soft MPI are removed in Template A and the hard jets become more correlated. This leads to an underestimation of $f_{\text{DP}}^{(\text{MC})}$. Conversely, at high p_T^{max} , genuine $W_0 + 2j_{\text{DPI}}$ events are not removed when constructing Template A, also leading to an underestimation of the extracted $f_{\text{DP}}^{(\text{MC})}$. These two competing effects are visible in figure 5, which shows $f_{\text{DP}}^{(\text{MC})}$ extracted as p_T^{max} is varied, along with the value of $f_{\text{DP}}^{(P)}$, as defined in equation (16). Therefore, the fit with the best agreement between $f_{\text{DP}}^{(P)}$ and $f_{\text{DP}}^{(\text{MC})}$ determines the value of $p_T^{\text{max}} = 15 \text{ GeV}$ chosen as default for the construction of Template A in this analysis. In this case, the value of $f_{\text{DP}}^{(P)}$, as defined in equation (16) (and indicated by the dotted line in figure 5), is within 10% of the value $f_{\text{DP}}^{(\text{MC})}(\Delta_{\text{jets}}^n) = 0.059 \pm 0.007$ obtained from the templates fit. This implies that, when using the optimal p_T^{max} derived above, the value of $f_{\text{DP}}^{(\text{MC})}$ (and therefore $f_{\text{DP}}^{(D)}$) can be regarded as a measurement at the parton level with an associated 10% uncertainty.

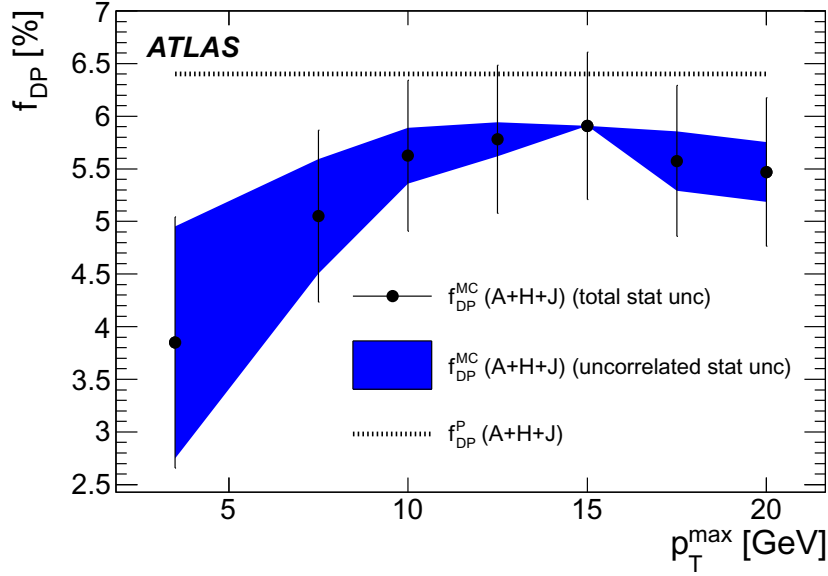


Figure 5. Variation of the extracted fraction of double-parton scattering from the Δ_{jets}^n distribution in the A + H + J MC simulation, $f_{\text{DP}}^{\text{(MC)}}$ (black points), as a function of the transverse momentum cut imposed on the scattered partons, p_T^{\max} . The band illustrates the statistical component of the uncertainty of $f_{\text{DP}}^{\text{(MC)}}$, relative to the reference sample with $p_T^{\max} = 15$ GeV, estimated by subtracting the statistical uncertainty of the reference sample in quadrature. The value, $f_{\text{DP}}^{\text{(P)}}$, of the fraction of double-parton scattering obtained directly at the parton level (see equation (16)) is also shown as a dashed line.

7.5. Model dependence of Template A

The effect of generator modelling is found by comparing the results for $f_{\text{DP}}^{\text{(MC)}}$, when SHERPA is used to provide Template A, $f_{\text{DP}}^{\text{(S)}}$, rather than A + H + J, $f_{\text{DP}}^{\text{(AHJ)}}$. In this case for the A + H + J sample, the p_T^{\max} parameter was set to 3.5 GeV to keep the samples comparable. The results of these fits, after applying the pile-up correction $r_{\text{pile-up}}$, are $f_{\text{DP}}^{\text{(S)}} = 0.031 \pm 0.008$ and $f_{\text{DP}}^{\text{(AHJ)}} = 0.034 \pm 0.006$. The quoted uncertainties are statistical and correlated between the two. However, the difference is smaller than either of the uncertainties and thus the results are consistent. The results of the two fits to the inclusive A + H + J sample are shown in figure 6.

7.5.1. Extraction of $f_{\text{DP}}^{\text{(D)}}$. Turning now to the data itself, the backgrounds are subtracted using the MC and data-driven estimates of section 6.1. The parameter $f_{\text{DP}}^{\text{(D)}}$ was extracted from a fit to the distribution of Δ_{jets}^n in the data sample of W+2-jet events after this physics background subtraction. After applying the pile-up correction $r_{\text{pile-up}}$, this yields

$$f_{\text{DP}}^{\text{(D)}}(\Delta_{\text{jets}}^n) = 0.076 \pm 0.013 \text{ (stat.)}, \quad (17)$$

with $\chi^2/N_{\text{dof}} = 37/28$. The result quoted above is in good agreement with the result of a fit to the distribution of Δ_{jets}^n . The resulting distributions obtained with $f_{\text{DP}}^{\text{(D)}}(\Delta_{\text{jets}}^n)$ are shown in figure 7.

The systematic uncertainties on this extracted value of $f_{\text{DP}}^{\text{(D)}}$ are discussed in the following.

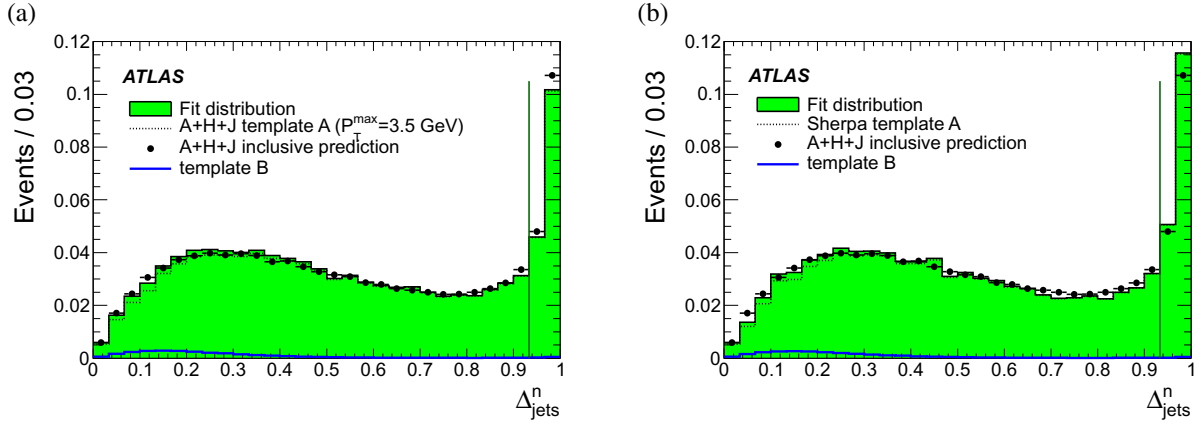


Figure 6. Distribution of Δ_{jets}^n in the inclusive A + H + J pseudo-data (dots). (a) A + H + J with $p_T^{\text{max}} = 3.5 \text{ GeV}$ and (b) SHERPA were used to provide Template A. Other details are as in the caption to figure 4.

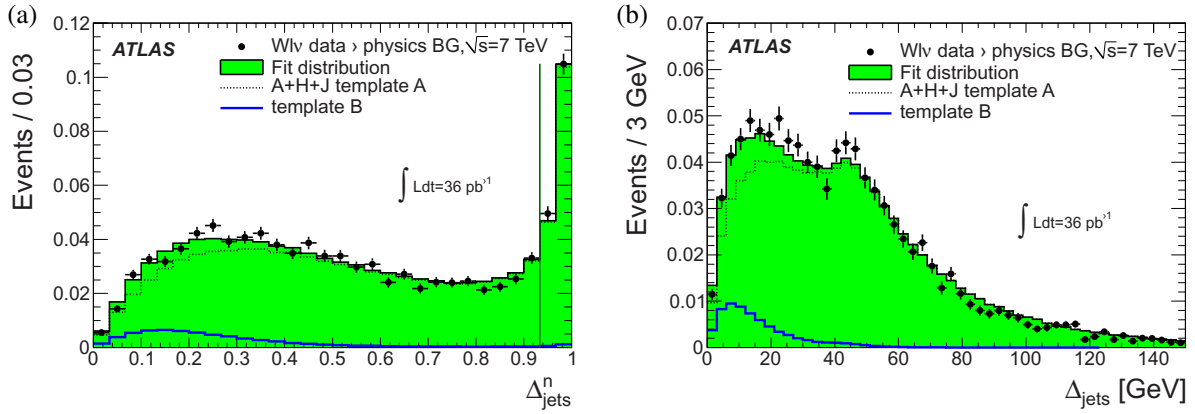


Figure 7. Distribution of (a) Δ_{jets}^n and (b) Δ_{jets} in the background-subtracted data (dots) compared to the result from the best fit for $f_{\text{DP}}^{(\text{D})}(\Delta_{\text{jets}}^n)$. The result is shown as the green histogram. In (a), the bins to the right of the vertical dash-dotted line were excluded from the fit. Data and the overall fit have been normalized to unity, Template A (dashed line) to $1 - f_{\text{DP}}^{(\text{D})}(\Delta_{\text{jets}}^n)$ and Template B (blue solid line) to $f_{\text{DP}}^{(\text{D})}(\Delta_{\text{jets}}^n)$.

7.5.2. Theoretical uncertainty. The uncertainty due to generator modelling is estimated by comparing the results for $f_{\text{DP}}^{(\text{S})}$ with $f_{\text{DP}}^{(\text{AHJ})}$. To be conservative, the statistical uncertainty on $f_{\text{DP}}^{(\text{S})}$ is propagated as a symmetric systematic uncertainty on $f_{\text{DP}}^{(\text{D})}$ due to the modelling. An additional uncertainty is due to the choice of p_T^{max} . The systematic uncertainty due to the variation of this value is obtained by demanding that $f_{\text{DP}}^{(\text{MC})}$ and $f_{\text{DP}}^{(\text{P})}$ are consistent within statistical uncertainties. From figure 5, upward and downward variations of p_T^{max} by 2.5 and 5 GeV, respectively, are deduced. The value of p_T^{max} was varied by these two amounts, resulting in a variation in $f_{\text{DP}}^{(\text{MC})}$ of 0.003. The two uncertainties discussed above were added in quadrature to estimate the total theoretical uncertainty of 0.004.

7.5.3. Jet energy scale and resolution. The overall impact of the jet energy scale on $f_{\text{DP}}^{(\text{D})}$ was determined by shifting the jet energy upwards and downwards in the MC samples by the jet energy scale uncertainty [46] and repeating the fit. The variations were found to be +0.009 and -0.008 , respectively. The larger of these two was symmetrized to provide the systematic uncertainty on $f_{\text{DP}}^{(\text{D})}$ due to that on the jet energy scale. Similarly, the overall impact of the jet energy resolution on $f_{\text{DP}}^{(\text{D})}$ was determined by degrading the jet energy resolution in the MC samples by the jet energy resolution uncertainty, and re-performing the fit. The variation in $f_{\text{DP}}^{(\text{D})}$ in this case, assumed to be symmetric, was found to be 0.005.

7.5.4. Physics backgrounds and lepton response. The impact of both physics background modelling and lepton response was considered via a direct comparison of $f_{\text{DP}}^{(\text{D})}$ obtained separately in the $W \rightarrow e\nu$ and $W \rightarrow \mu\nu$ channels. Half of the obtained difference, which was at the sub-per cent level, was taken as a measure of the associated uncertainty. The uncertainty associated with background subtraction was also determined by varying the background normalization and shape. The multi-jet background shape was varied in both channels by using MC instead of data-driven methods to estimate it, with no reversal of cuts. The shift in $f_{\text{DP}}^{(\text{D})}$ in this case was -0.001 . The normalization of the multi-jet background was varied in the $W \rightarrow e\nu$ channel by taking the relative normalization of the background contribution from two independent methods of background estimation—this led to a relative variation of about 50%. For the $W \rightarrow \mu\nu$ channel, in which multi-jet background is better understood, a fractional shift of 20% was assumed in the background normalization. The shift in $f_{\text{DP}}^{(\text{D})}$ when the multi-jet background normalization was increased was found to be +0.008. The uncertainty associated with the normalization of electroweak and top backgrounds was evaluated by increasing the predicted cross sections of these processes by their theoretical uncertainty of 5% [41], resulting in a +0.001 variation in $f_{\text{DP}}^{(\text{D})}$. Symmetrizing and then adding these uncertainties in quadrature yields the total uncertainty due to physics backgrounds and lepton response on $f_{\text{DP}}^{(\text{D})}$ of 0.008.

7.5.5. Pile-up. The systematic uncertainty due to this effect was evaluated by propagating the statistical uncertainty on the pile-up correction, $r_{\text{pile-up}}$, as determined in section 7.2, resulting in an uncertainty on $f_{\text{DP}}^{(\text{D})}$ of 0.010.

7.5.6. Impact of $W + 1$ jet. It was verified that the contribution of $W + 1$ -jet configurations from the hardest scatter supplemented with a single jet from a secondary scatter formed a negligible contribution to the DPI rate at parton level, as well as in the modelling of Template A.

The individual contributions to the systematic uncertainty on $f_{\text{DP}}^{(\text{D})}$ are summarized in table 1. The contributions are added in quadrature, yielding

$$f_{\text{DP}}^{(\text{D})} = 0.076 \pm 0.013 \text{ (stat.)} \pm 0.018 \text{ (sys.)}. \quad (18)$$

The extracted value of $f_{\text{DP}}^{(\text{D})}$ is consistent with the value of $f_{\text{DP}}^{(\text{MC})}$ extracted in section 7, within the quoted uncertainties and hence with $f_{\text{DP}}^{(\text{P})}$ at the parton level, as discussed in section 7.3. This implies that the MC models studied in the analysis describe the rate and kinematics of the DPI contribution well.

Table 1. Summary of the fractional uncertainties on $f_{\text{DP}}^{(\text{D})}$.

Systematic source	Uncertainty (%)
Theory	10
Pile-up	13
Jet energy scale	12
Jet energy resolution	8
Background modelling and lepton response	11
Total systematic	24
Total statistical	17

8. Hadron-level studies

Since σ_{eff} and $f_{\text{DP}}^{(\text{P})}$ are intrinsically parton-level quantities, they are not directly observable. Conversely, $f_{\text{DP}}^{(\text{D})}$ contains residual dependencies on detector resolutions and efficiencies. This renders a direct comparison with theoretical models impossible. To allow the results of this study to be used for comparisons with MPI models in the future, the key distributions have been corrected for detector effects to the final-state hadron level. The hadron-level requirements mirror the selection described in section 5, except that cuts were applied to hadron-level quantities in MC simulation. Hadron-level jets were constructed by running the same jet finder as for the detector level, using all final-state hadron-level particles with lifetimes longer than 30 ps as input, with the neutrinos and the charged leptons originating from the decay of the W bosons being excluded. Jets were defined with the anti- k_t algorithm with $p_{\text{T}} > 20$ GeV, $|y| < 2.8$ and $R = 0.4$. In addition, jets within a distance of $\Delta R = 0.5$ from the leptons were removed. Dijet events were required to contain exactly two jets, reconstructed using the same algorithm, input objects and kinematic selection as already described. The $\Delta_{\text{jets}}^{\text{n}}$ and Δ_{jets} distributions in $W + 2$ -jet data unfolded to the hadron level are shown in figure 8. The background-subtracted data has been corrected, using a Bayesian unfolding algorithm, to the hadron level using the RooUnfold package [59]. The response matrix used to unfold the data was trained on A + H + J predictions and two iterations were used to converge to the unfolded distributions, resulting in a smoother distribution than that seen at detector level. The unfolded results are compared with both A + H + J and SHERPA MC predictions directly obtained at hadron level.

The systematic uncertainties on the $\Delta_{\text{jets}}^{\text{n}}$ and Δ_{jets} distributions were obtained by repeating the studies outlined in section 7.5.1 with the exception of pile-up uncertainty. The latter was estimated by comparing the background-subtracted, corrected data distributions measured at hadron level with that obtained when rejecting all events other than those with exactly one primary vertex selected as described in section 5. The uncertainty due to the unfolding procedure itself was estimated as the shift in the corrected data distribution when SHERPA instead of A + H + J was used to train the response matrix. The overall uncertainty on the unfolded distribution was found, per bin of the distribution, by a quadrature sum of the uncertainties described above and is dominated by the pile-up uncertainty. For completeness, the unfolded $\Delta_{\text{jets}}^{\text{n}}$ and Δ_{jets} distributions are compared with a linear combination of Template A from A + H + J and Template B from PYTHIA6, both at the hadron level, in proportions determined by the value of $f_{\text{DP}}^{(\text{D})}$, as shown in figure 9. Perfect agreement between $f_{\text{DP}}^{(\text{D})}$ and its hadron-level equivalent is not expected as the phase space at hadron level, covered by the $W+2$ -jet sample

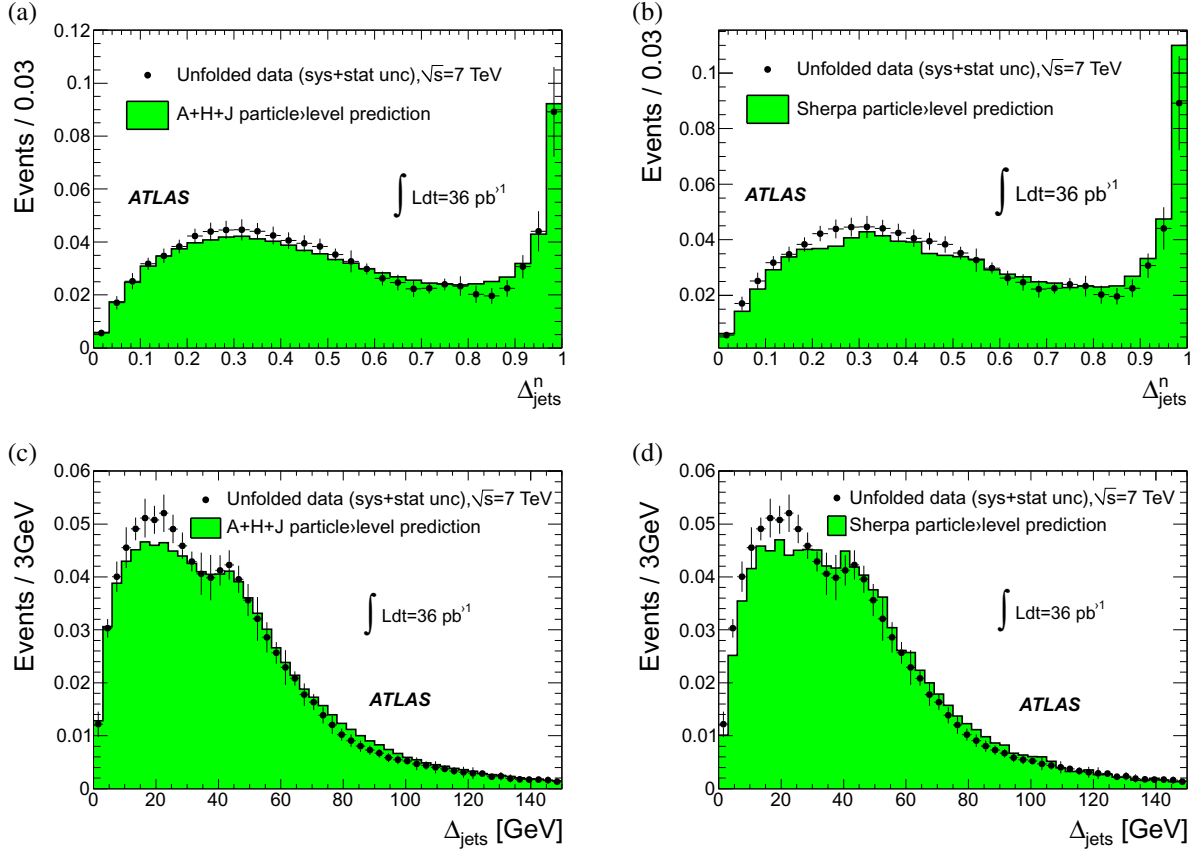


Figure 8. Distributions of (a), (b) Δ_{jets}^n and (c), (d) Δ_{jets} in the data after unfolding to hadron level (dots) compared to MC expectations from (a), (c) A + H + J and (b), (d) SHERPA at the hadron level (green histogram). The error bars represent the quadrature sum of systematic and statistical uncertainties on each bin, and both histograms have been normalized to unity.

at detector level used for the determination of $f_{\text{DP}}^{(\text{D})}$, is not exactly the same as for the unfolded distribution. The value of $f_{\text{DP}}^{(\text{D})}$ determined directly via a fit at the hadron level was found to be within 10% of the value determined at detector level.

8.1. Determination of σ_{eff}

The value of σ_{eff} is related to $f_{\text{DP}}^{(\text{D})}$ through equation (9). The additional input of the exclusivity ratio, $N_{W_{0j}}/N_{W_{+2j}} = 23$, is evaluated from the event yields in the selected $W + 2$ -jet and $W + 0$ -jet samples. The associated statistical uncertainty is at the 2% level. Additionally, the number of dijet events $N_{2j} = 9488$ is obtained from the event yield in the early period of 2010 data taking, corresponding to an integrated luminosity of $\mathcal{L}_{2j} = 184 \mu\text{b}^{-1}$. In this period of data taking, the trigger selection for dijet events was measured to be fully efficient ($\varepsilon_{2j} = 1$) [46]. A further correction to N_{2j} was made for lepton–jet overlap removal, which was applied to the jets when constructing Template A but not in Template B. It was evaluated by applying overlap removal for jets in Template B, giving a correction factor of 0.96.

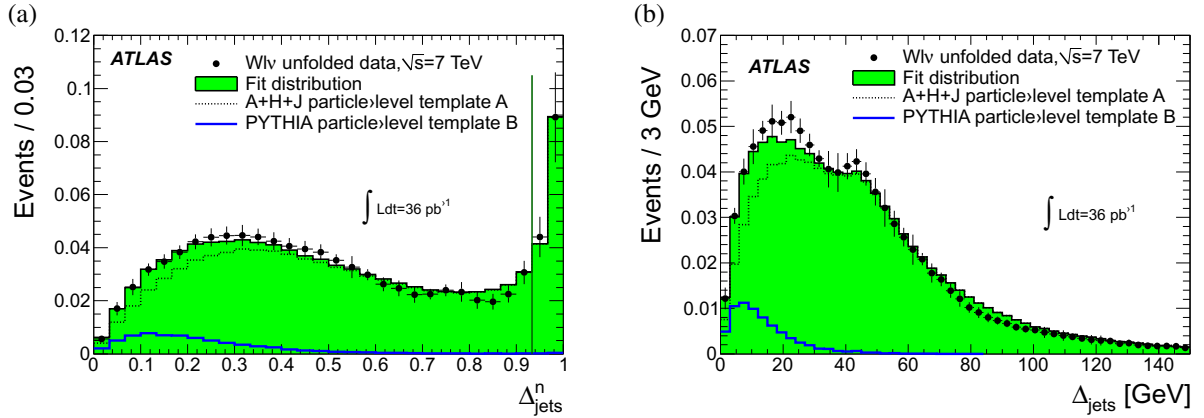


Figure 9. Distributions of (a) Δ_{jets}^n and (b) Δ_{jets} in the data after unfolding to hadron level (dots) compared to the results of a linear combination with $f_{\text{DP}}^{(\text{D})}$ (green histogram) of Template A extracted from A+H+J hadron-level simulation (dashed line) and of Template B obtained from the PYTHIA6 hadron-level simulation (solid blue line). The error bars on the data represent the quadrature sum of the statistical and systematic uncertainties. Data and the overall fit have been normalized to unity, Template A to $1 - f_{\text{DP}}^{(\text{D})}(\Delta_{\text{jets}}^n)$ and Template B to $f_{\text{DP}}^{(\text{D})}(\Delta_{\text{jets}}^n)$.

Table 2. Summary of fractional systematic uncertainties on σ_{eff} .

Systematic source	Uncertainty (%)
$f_{\text{DP}}^{(\text{D})}$	24
Background and lepton response	5
Luminosity	3
Total systematic	+33 -20
Total statistical	17

The systematic uncertainties are summarized in table 2, with the following breakdown of their origins:

- The uncertainties on $f_{\text{DP}}^{(\text{D})}$ —determined in section 7.5.1—are propagated asymmetrically to σ_{eff} .
- Physics backgrounds and response to leptons—the impact of the lepton energy response and background normalization uncertainties were considered by propagating the uncertainty on $f_{\text{DP}}^{(\text{D})}$ obtained for this effect. In addition, the impact of lepton scale and the background normalization uncertainties on the exclusivity ratio, N_{W_0}/N_{W+2j} , were included.
- Acceptance and response cancellation—equation (8) is the result of factorization which implies that the kinematics of the lepton and DPI system are not correlated, either in terms of geometrical acceptance or through detector response. Apart from the effect of

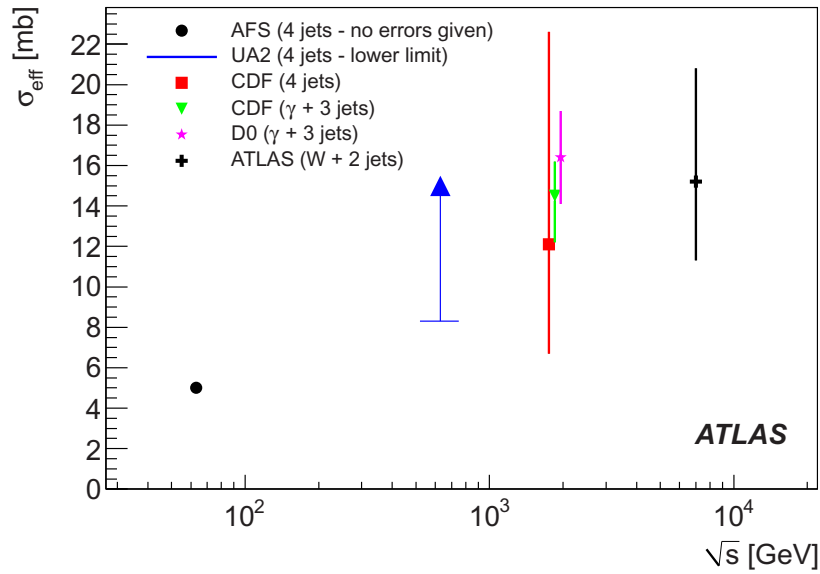


Figure 10. The centre-of-mass energy, \sqrt{s} , dependence of σ_{eff} extracted in different processes in different experiments. An offset has been applied to the 1.8 TeV data points in order to distinguish them. The error bars on the data points represent the statistical and systematic uncertainties added in quadrature.

lepton–jet overlap removal, which was discussed above, various sources of uncertainty on this assumption were considered and found to be negligible.

The above leads to a measured central value of

$$\sigma_{\text{eff}}(7 \text{ TeV}) = 15 \pm 3 \text{ (stat.) } {}^{+5}_{-3} \text{ (syst.) mb.} \quad (19)$$

Assuming factorization, this value of σ_{eff} is consistent with values previously measured in other experiments at lower centre-of-mass [15–19], as can be seen in figure 10.

9. Conclusions

The double-parton interaction rate $f_{\text{DP}}^{(\text{D})}$ in events with a W boson and exactly two jets in the final state has been extracted in pp collisions at a centre-of-mass energy of $\sqrt{s} = 7 \text{ TeV}$ using data corresponding to an integrated luminosity of 36 pb^{-1} . For jets with transverse momentum $p_{\text{T}} > 20 \text{ GeV}$ and rapidity $|y| < 2.8$, in the ATLAS detector at the LHC, a central value of

$$f_{\text{DP}}^{(\text{D})} = 0.08 \pm 0.01 \text{ (stat.) } \pm 0.02 \text{ (sys.)}$$

is obtained. In terms of measured rate and kinematics of the dijet system there is good agreement with the predictions of the MC models studied in the analysis. The result for $f_{\text{DP}}^{(\text{D})}$ is used to extract the parameter σ_{eff} through the production of $W + 2$ -jet events. The value extracted from data is

$$\sigma_{\text{eff}}(7 \text{ TeV}) = 15 \pm 3 \text{ (stat.) } {}^{+5}_{-3} \text{ (sys.) mb.}$$

This value is consistent with values previously measured in other experiments at lower centre-of-mass energies.

Acknowledgments

We thank CERN for the very successful operation of the LHC, as well as the support staff from our institutions without whom ATLAS could not be operated efficiently. We acknowledge the support of ANPCyT, Argentina; YerPhI, Armenia; ARC, Australia; BMWF and FWF, Austria; ANAS, Azerbaijan; SSTC, Belarus; CNPq and FAPESP, Brazil; NSERC, NRC and CFI, Canada; CERN; CONICYT, Chile; CAS, MOST and NSFC, China; COLCIENCIAS, Colombia; MSMT CR, MPO CR and VSC CR, Czech Republic; DNRF, DNSRC and Lundbeck Foundation, Denmark; EPLANET, ERC and NSRF, European Union; IN2P3-CNRS, CEA-DSM/IRFU, France; GNSF, Georgia; BMBF, DFG, HGF, MPG and AvH Foundation, Germany; GSRT and NSRF, Greece; ISF, MINERVA, GIF, DIP and Benoziyo Center, Israel; INFN, Italy; MEXT and JSPS, Japan; CNRST, Morocco; FOM and NWO, Netherlands; BRF and RCN, Norway; MNiSW, Poland; GRICES and FCT, Portugal; MERYS (MECTS), Romania; MES of Russia and ROSATOM, Russian Federation; JINR; MSTD, Serbia; MSSR, Slovakia; ARRS and MVZT, Slovenia; DST/NRF, South Africa; MICINN, Spain; SRC and Wallenberg Foundation, Sweden; SER, SNSF and Cantons of Bern and Geneva, Switzerland; NSC, Taiwan; TAEK, Turkey; STFC, the Royal Society and Leverhulme Trust, UK; DOE and NSF, USA. The crucial computing support from all WLCG partners is acknowledged gratefully, in particular from CERN and the ATLAS Tier-1 facilities at TRIUMF (Canada), NDGF (Denmark, Norway, Sweden), CC-IN2P3 (France), KIT/GridKA (Germany), INFN-CNAF (Italy), NL-T1 (Netherlands), PIC (Spain), ASGC (Taiwan), RAL (UK) and BNL (USA) and in the Tier-2 facilities worldwide.

The ATLAS Collaboration

G Aad⁴⁸, T Abajyan²¹, B Abbott¹¹¹, J Abdallah¹², S Abdel Khalek¹¹⁵, A A Abdelalim⁴⁹, O Abdinov¹¹, R Aben¹⁰⁵, B Abi¹¹², M Abolins⁸⁸, O S AbouZeid¹⁵⁸, H Abramowicz¹⁵³, H Abreu¹³⁶, M I Ochoa⁷⁷, B S Acharya^{164a,164b,179}, L Adamczyk³⁸, D L Adams²⁵, T N Addy⁵⁶, J Adelman¹⁷⁶, S Adomeit⁹⁸, P Adragna⁷⁵, T Adye¹²⁹, S Aefsky²³, J A Aguilar-Saavedra^{124b,180}, M Agustoni¹⁷, S P Ahlen²², F Ahles⁴⁸, A Ahmad¹⁴⁸, M Ahsan⁴¹, G Aielli^{133a,133b}, T P A Åkesson⁷⁹, G Akimoto¹⁵⁵, A V Akimov⁹⁴, M A Alam⁷⁶, J Albert¹⁶⁹, S Albrand⁵⁵, M Aleksa³⁰, I N Aleksandrov⁶⁴, F Alessandria^{89a}, C Alexa^{26a}, G Alexander¹⁵³, G Alexandre⁴⁹, T Alexopoulos¹⁰, M Alhroob^{164a,164c}, M Aliev¹⁶, G Alimonti^{89a}, J Alison¹²⁰, B M M Allbrooke¹⁸, L J Allison⁷¹, P P Allport⁷³, S E Allwood-Spiers⁵³, J Almond⁸², A Aloisio^{102a,102b}, R Alon¹⁷², A Alonso³⁶, F Alonso⁷⁰, A Altheimer³⁵, B Alvarez Gonzalez⁸⁸, M G Alviggi^{102a,102b}, K Amako⁶⁵, C Amelung²³, V V Ammosov^{128,218}, S P Amor Dos Santos^{124a}, A Amorim^{124a,181}, S Amoroso⁴⁸, N Amram¹⁵³, C Anastopoulos³⁰, L S Ancu¹⁷, N Andari¹¹⁵, T Andeen³⁵, C F Anders^{58b}, G Anders^{58a}, K J Anderson³¹, A Andreatza^{89a,89b}, V Andrei^{58a}, X S Anduaga⁷⁰, S Angelidakis⁹, P Anger⁴⁴, A Angerami³⁵, F Anghinolfi³⁰, A Anisenkov¹⁰⁷, N Anjos^{124a}, A Annovi⁴⁷, A Antonaki⁹, M Antonelli⁴⁷, A Antonov⁹⁶, J Antos^{144b}, F Anulli^{132a}, M Aoki¹⁰¹, S Aoun⁸³, L Aperio Bella⁵, R Apolle^{118,182}, G Arabidze⁸⁸, I Aracena¹⁴³, Y Arai⁶⁵, A T H Arce⁴⁵, S Arfaoui¹⁴⁸, J-F Arguin⁹³, S Argyropoulos⁴², E Arik^{19a,218}, M Arik^{19a}, A J Armbruster⁸⁷, O Arnaez⁸¹, V Arnal⁸⁰, A Artamonov⁹⁵, G Artoni^{132a,132b}, D Arutinov²¹, S Asai¹⁵⁵, S Ask²⁸, B Åsman^{146a,146b}, L Asquith⁶, K Assamagan^{25,183}, R Astalos^{144a}, A Astbury¹⁶⁹, M Atkinson¹⁶⁵, B Auerbach⁶, E Auge¹¹⁵, K Augsten¹²⁶, M Aourousseau^{145a}, G Avolio³⁰, D Axen¹⁶⁸, G Azuelos^{93,184}, Y Azuma¹⁵⁵, M A Baak³⁰, G Baccaglioni^{89a}, C Bacci^{134a,134b}, A M Bach¹⁵,

H Bachacou¹³⁶, K Bachas¹⁵⁴, M Backes⁴⁹, M Backhaus²¹, J Backus Mayes¹⁴³, E Badesu^{26a}, P Bagnaia^{132a,132b}, Y Bai^{33a}, D C Bailey¹⁵⁸, T Bain³⁵, J T Baines¹²⁹, O K Baker¹⁷⁶, S Baker⁷⁷, P Balek¹²⁷, F Balli¹³⁶, E Banas³⁹, P Banerjee⁹³, Sw Banerjee¹⁷³, D Banfi³⁰, A Bangert¹⁵⁰, V Bansal¹⁶⁹, H S Bansil¹⁸, L Barak¹⁷², S P Baranov⁹⁴, T Barber⁴⁸, E L Barberio⁸⁶, D Barberis^{50a,50b}, M Barbero⁸³, D Y Bardin⁶⁴, T Barillari⁹⁹, M Barisonzi¹⁷⁵, T Barklow¹⁴³, N Barlow²⁸, B M Barnett¹²⁹, R M Barnett¹⁵, A Baroncelli^{134a}, G Barone⁴⁹, A J Barr¹¹⁸, F Barreiro⁸⁰, J Barreiro Guimarães da Costa⁵⁷, R Bartoldus¹⁴³, A E Barton⁷¹, V Bartsch¹⁴⁹, A Basye¹⁶⁵, R L Bates⁵³, L Batkova^{144a}, J R Batley²⁸, A Battaglia¹⁷, M Battistin³⁰, F Bauer¹³⁶, H S Bawa^{143,185}, S Beale⁹⁸, T Beau⁷⁸, P H Beauchemin¹⁶¹, R Beccherle^{50a}, P Bechtel²¹, H P Beck¹⁷, K Becker¹⁷⁵, S Becker⁹⁸, M Beckingham¹³⁸, K H Becks¹⁷⁵, A J Beddall^{19c}, A Beddall^{19c}, S Bedikian¹⁷⁶, V A Bednyakov⁶⁴, C P Bee⁸³, L J Beemster¹⁰⁵, M Begel²⁵, S Behar Harpaz¹⁵², C Belanger-Champagne⁸⁵, P J Bell⁴⁹, W H Bell⁴⁹, G Bella¹⁵³, L Bellagamba^{20a}, M Bellomo³⁰, A Belloni⁵⁷, O Beloborodova^{107,186}, K Belotskiy⁹⁶, O Beltramello³⁰, O Benary¹⁵³, D Bencheekroun^{135a}, K Bendtz^{146a,146b}, N Benekos¹⁶⁵, Y Benhammou¹⁵³, E Benhar Noccioli⁴⁹, J A Benitez Garcia^{159b}, D P Benjamin⁴⁵, M Benoit¹¹⁵, J R Bensinger²³, K Benslama¹³⁰, S Bentvelsen¹⁰⁵, D Berge³⁰, E Bergeaas Kuutmann⁴², N Berger⁵, F Berghaus¹⁶⁹, E Berglund¹⁰⁵, J Beringer¹⁵, P Bernat⁷⁷, R Bernhard⁴⁸, C Bernius²⁵, F U Bernlochner¹⁶⁹, T Berry⁷⁶, C Bertella⁸³, A Bertin^{20a,20b}, F Bertolucci^{122a,122b}, M I Besana^{89a,89b}, G J Besjes¹⁰⁴, N Besson¹³⁶, S Bethke⁹⁹, W Bhimji⁴⁶, R M Bianchi³⁰, L Bianchini²³, M Bianco^{72a,72b}, O Biebel⁹⁸, S P Bieniek⁷⁷, K Bierwagen⁵⁴, J Biesiada¹⁵, M Biglietti^{134a}, H Bilokon⁴⁷, M Bindi^{20a,20b}, S Binet¹¹⁵, A Bingul^{19c}, C Bini^{132a,132b}, C Biscarat¹⁷⁸, B Bittner⁹⁹, C W Black¹⁵⁰, J E Black¹⁴³, K M Black²², R E Blair⁶, J-B Blanchard¹³⁶, T Blazek^{144a}, I Bloch⁴², C Blocker²³, J Blocki³⁹, W Blum⁸¹, U Blumenschein⁵⁴, G J Bobbink¹⁰⁵, V S Bobrovnikov¹⁰⁷, S S Bocchetta⁷⁹, A Bocci⁴⁵, C R Boddy¹¹⁸, M Boehler⁴⁸, J Boek¹⁷⁵, T T Boek¹⁷⁵, N Boelaert³⁶, J A Bogaerts³⁰, A Bogdanchikov¹⁰⁷, A Bogouch^{90,218}, C Bohm^{146a}, J Bohm¹²⁵, V Boisvert⁷⁶, T Bold³⁸, V Boldea^{26a}, N M Bolnet¹³⁶, M Bomben⁷⁸, M Bona⁷⁵, M Boonekamp¹³⁶, S Bordini⁷⁸, C Borer¹⁷, A Borisov¹²⁸, G Borissov⁷¹, I Borjanovic^{13a}, M Borri⁸², S Borroni⁴², J Bortfeldt⁹⁸, V Bortolotto^{134a,134b}, K Bos¹⁰⁵, D Boscherini^{20a}, M Bosman¹², H Boterenbrood¹⁰⁵, J Bouchami⁹³, J Boudreau¹²³, E V Bouhova-Thacker⁷¹, D Boumediene³⁴, C Bourdarios¹¹⁵, N Bousson⁸³, S Boutouil^{135d}, A Boveia³¹, J Boyd³⁰, I R Boyko⁶⁴, I Bozovic-Jelisavcic^{13b}, J Bracinik¹⁸, P Branchini^{134a}, A Brandt⁸, G Brandt¹¹⁸, O Brandt⁵⁴, U Bratzler¹⁵⁶, B Brau⁸⁴, J E Brau¹¹⁴, H M Braun^{175,218}, S F Brazzale^{164a,164c}, B Brelier¹⁵⁸, J Bremer³⁰, K Brendlinger¹²⁰, R Brenner¹⁶⁶, S Bressler¹⁷², T M Bristow^{145b}, D Britton⁵³, F M Brochu²⁸, I Brock²¹, R Brock⁸⁸, F Broggi^{89a}, C Bromberg⁸⁸, J Bronner⁹⁹, G Brooijmans³⁵, T Brooks⁷⁶, W K Brooks^{32b}, G Brown⁸², P A Bruckman de Renstrom³⁹, D Bruncko^{144b}, R Bruneliere⁴⁸, S Brunet⁶⁰, A Bruni^{20a}, G Bruni^{20a}, M Bruschi^{20a}, L Bryngemark⁷⁹, T Buanes¹⁴, Q Buat⁵⁵, F Bucci⁴⁹, J Buchanan¹¹⁸, P Buchholz¹⁴¹, R M Buckingham¹¹⁸, A G Buckley⁴⁶, S I Buda^{26a}, I A Budagov⁶⁴, B Budick¹⁰⁸, V Büscher⁸¹, L Bugge¹¹⁷, O Bulekov⁹⁶, A C Bundock⁷³, M Bunse⁴³, T Buran¹¹⁷, H Burckhart³⁰, S Burdin⁷³, T Burgess¹⁴, S Burke¹²⁹, E Busato³⁴, P Bussey⁵³, C P Buszello¹⁶⁶, B Butler¹⁴³, J M Butler²², C M Buttar⁵³, J M Butterworth⁷⁷, W Buttinger²⁸, M Byszewski³⁰, S Cabrera Urbán¹⁶⁷, D Caforio^{20a,20b}, O Cakir^{4a}, P Calafiura¹⁵, G Calderini⁷⁸, P Calfayan⁹⁸, R Calkins¹⁰⁶, L P Caloba^{24a}, R Caloi^{132a,132b}, D Calvet³⁴, S Calvet³⁴, R Camacho Toro³⁴, P Camarri^{133a,133b}, D Cameron¹¹⁷, L M Caminada¹⁵, R Caminal Armadans¹², S Campana³⁰, M Campanelli⁷⁷, V Canale^{102a,102b}, F Canelli³¹, A Canepa^{159a}, J Cantero⁸⁰, R Cantrill⁷⁶, T Cao⁴⁰, M D M Capeans Garrido³⁰, I Caprini^{26a}, M Caprini^{26a}, D Capriotti⁹⁹, M Capua^{37a,37b},

R Caputo⁸¹, R Cardarelli^{133a}, T Carli³⁰, G Carlino^{102a}, L Carminati^{89a,89b}, S Caron¹⁰⁴, E Carquin^{32b}, G D Carrillo-Montoya^{145b}, A A Carter⁷⁵, J R Carter²⁸, J Carvalho^{124a,187}, D Casadei¹⁰⁸, M P Casado¹², M Cascella^{122a,122b}, C Caso^{50a,50b,218}, E Castaneda-Miranda¹⁷³, V Castillo Gimenez¹⁶⁷, N F Castro^{124a}, G Cataldi^{72a}, P Catastini⁵⁷, A Catinaccio³⁰, J R Catmore³⁰, A Cattai³⁰, G Cattani^{133a,133b}, S Caughron⁸⁸, V Cavaliere¹⁶⁵, P Cavalleri⁷⁸, D Cavalli^{89a}, M Cavalli-Sforza¹², V Cavasinni^{122a,122b}, F Ceradini^{134a,134b}, A S Cerqueira^{24b}, A Cerri¹⁵, L Cerrito⁷⁵, F Cerutti¹⁵, S A Cetin^{19b}, A Chafaq^{135a}, D Chakraborty¹⁰⁶, I Chalupkova¹²⁷, K Chan³, P Chang¹⁶⁵, B Chapleau⁸⁵, J D Chapman²⁸, J W Chapman⁸⁷, D G Charlton¹⁸, V Chavda⁸², C A Chavez Barajas³⁰, S Cheatham⁸⁵, S Chekanov⁶, S V Chekulaev^{159a}, G A Chelkov⁶⁴, M A Chelstowska¹⁰⁴, C Chen⁶³, H Chen²⁵, S Chen^{33c}, X Chen¹⁷³, Y Chen³⁵, Y Cheng³¹, A Cheplakov⁶⁴, R Cherkaoui El Moursli^{135e}, V Chernyatin²⁵, E Cheu⁷, S L Cheung¹⁵⁸, L Chevalier¹³⁶, G Chiefari^{102a,102b}, L Chikovani^{51a,218}, J T Childers³⁰, A Chilingarov⁷¹, G Chiodini^{72a}, A S Chisholm¹⁸, R T Chislett⁷⁷, A Chitan^{26a}, M V Chizhov⁶⁴, G Choudalakis³¹, S Chouridou⁹, B K B Chow⁹⁸, I A Christidi⁷⁷, A Christov⁴⁸, D Chromek-Burckhart³⁰, M L Chu¹⁵¹, J Chudoba¹²⁵, G Ciapetti^{132a,132b}, A K Ciftci^{4a}, R Ciftci^{4a}, D Cinca⁶², V Cindro⁷⁴, A Ciocio¹⁵, M Cirilli⁸⁷, P Cirkovic^{13b}, Z H Citron¹⁷², M Citterio^{89a}, M Ciubancan^{26a}, A Clark⁴⁹, P J Clark⁴⁶, R N Clarke¹⁵, W Cleland¹²³, J C Clemens⁸³, B Clement⁵⁵, C Clement^{146a,146b}, Y Coadou⁸³, M Cobal^{164a,164c}, A Coccaro¹³⁸, J Cochran⁶³, L Coffey²³, J G Cogan¹⁴³, J Coggeshall¹⁶⁵, J Colas⁵, S Cole¹⁰⁶, A P Colijn¹⁰⁵, N J Collins¹⁸, C Collins-Tooth⁵³, J Collot⁵⁵, T Colombo^{119a,119b}, G Colon⁸⁴, G Compostella⁹⁹, P Conde Muiño^{124a}, E Coniavitis¹⁶⁶, M C Conidi¹², S M Consonni^{89a,89b}, V Consorti⁴⁸, S Constantinescu^{26a}, C Conta^{119a,119b}, G Conti⁵⁷, F Conventi^{102a,188}, M Cooke¹⁵, B D Cooper⁷⁷, A M Cooper-Sarkar¹¹⁸, K Copic¹⁵, T Cornelissen¹⁷⁵, M Corradi^{20a}, F Corriveau^{85,189}, A Cortes-Gonzalez¹⁶⁵, G Cortiana⁹⁹, G Costa^{89a}, M J Costa¹⁶⁷, D Costanzo¹³⁹, D Côté³⁰, G Cottin^{32a}, L Courneyea¹⁶⁹, G Cowan⁷⁶, B E Cox⁸², K Cranmer¹⁰⁸, F Crescioli⁷⁸, M Cristinziani²¹, G Crosetti^{37a,37b}, S Crépe-Renaudin⁵⁵, C-M Cuciuc^{26a}, C Cuenca Almenar¹⁷⁶, T Cuhadar Donszelmann¹³⁹, J Cummings¹⁷⁶, M Curatolo⁴⁷, C J Curtis¹⁸, C Cuthbert¹⁵⁰, P Cwetanski⁶⁰, H Czirr¹⁴¹, P Czodrowski⁴⁴, Z Czczyula¹⁷⁶, S D'Auria⁵³, M D'Onofrio⁷³, A D'Orazio^{132a,132b}, M J Da Cunha Sargedas De Sousa^{124a}, C Da Via⁸², W Dabrowski³⁸, A Dafinca¹¹⁸, T Dai⁸⁷, F Dallaire⁹³, C Dallapiccola⁸⁴, M Dam³⁶, D S Damiani¹³⁷, H O Danielsson³⁰, V Dao¹⁰⁴, G Darbo^{50a}, G L Darlea^{26b}, J A Dassoulas⁴², W Davey²¹, T Davidek¹²⁷, N Davidson⁸⁶, R Davidson⁷¹, E Davies^{118,182}, M Davies⁹³, O Davignon⁷⁸, A R Davison⁷⁷, Y Davygora^{58a}, E Dawe¹⁴², I Dawson¹³⁹, R K Daya-Ishmukhametova²³, K De⁸, R de Asmundis^{102a}, S De Castro^{20a,20b}, S De Cecco⁷⁸, J de Graat⁹⁸, N De Groot¹⁰⁴, P de Jong¹⁰⁵, C De La Taille¹¹⁵, H De la Torre⁸⁰, F De Lorenzi⁶³, L De Nooij¹⁰⁵, D De Pedis^{132a}, A De Salvo^{132a}, U De Sanctis^{164a,164c}, A De Santo¹⁴⁹, J B De Vivie De Regie¹¹⁵, G De Zorzi^{132a,132b}, W J Dearnaley⁷¹, R Debbe²⁵, C Debenedetti⁴⁶, B Dechenaux⁵⁵, D V Dedovich⁶⁴, J Degenhardt¹²⁰, J Del Peso⁸⁰, T Del Prete^{122a,122b}, T Delemontex⁵⁵, M Deliyergiyev⁷⁴, A Dell'Acqua³⁰, L Dell'Asta²², M Della Pietra^{102a,188}, D della Volpe^{102a,102b}, M Delmastro⁵, P A Delsart⁵⁵, C Deluca¹⁰⁵, S Demers¹⁷⁶, M Demichev⁶⁴, B Demirkoz^{12,190}, S P Denisov¹²⁸, D Derendarz³⁹, J E Derkaoui^{135d}, F Derue⁷⁸, P Dervan⁷³, K Desch²¹, P O Deviveiros¹⁰⁵, A Dewhurst¹²⁹, B DeWilde¹⁴⁸, S Dhaliwal¹⁵⁸, R Dhullipudi^{25,191}, A Di Ciaccio^{133a,133b}, L Di Ciaccio⁵, C Di Donato^{102a,102b}, A Di Girolamo³⁰, B Di Girolamo³⁰, S Di Luise^{134a,134b}, A Di Mattia¹⁵², B Di Micco³⁰, R Di Nardo⁴⁷, A Di Simone^{133a,133b}, R Di Sipio^{20a,20b}, M A Diaz^{32a}, E B Diehl⁸⁷, J Dietrich⁴², T A Dietzsch^{58a}, S Diglio⁸⁶, K Dindar Yagci⁴⁰, J Dingfelder²¹, F Dinul^{26a}, C Dionisi^{132a,132b}, P Dita^{26a}, S Dita^{26a}, F Dittus³⁰,

F Djama⁸³, T Djobava^{51b}, M A B do Vale^{24c}, A Do Valle Wemans^{124a,192}, T K O Doan⁵, M Dobbs⁸⁵, D Dobos³⁰, E Dobson⁷⁷, J Dodd³⁵, C Doglioni⁴⁹, T Doherty⁵³, Y Doi^{65,218}, J Dolejsi¹²⁷, Z Dolezal¹²⁷, B A Dolgoshein^{96,218}, T Dohmae¹⁵⁵, M Donadelli^{24d}, J Donini³⁴, J Dopke³⁰, A Doria^{102a}, A Dos Anjos¹⁷³, A Dotti^{122a,122b}, M T Dova⁷⁰, A D Doxiadis¹⁰⁵, A T Doyle⁵³, N Dressnandt¹²⁰, M Dris¹⁰, J Dubbert⁹⁹, S Dube¹⁵, E Dubreuil³⁴, E Duchovni¹⁷², G Duckeck⁹⁸, D Duda¹⁷⁵, A Dudarev³⁰, F Dudziak⁶³, M Dührssen³⁰, I P Duerdoth⁸², L Duflot¹¹⁵, M-A Dufour⁸⁵, L Duguid¹⁷⁶, M Dunford^{58a}, H Duran Yildiz^{4a}, R Duxfield¹³⁹, M Dwuznik³⁸, M Düren⁵², W L Ebenstein⁴⁵, J Ebke⁹⁸, S Eckweiler⁸¹, W Edson², C A Edwards⁷⁶, N C Edwards⁵³, W Ehrenfeld²¹, T Eifert¹⁴³, G Eigen¹⁴, K Einsweiler¹⁵, E Eisenhandler⁷⁵, T Ekelof¹⁶⁶, M El Kacimi^{135c}, M Ellert¹⁶⁶, S Elles⁵, F Ellinghaus⁸¹, K Ellis⁷⁵, N Ellis³⁰, J Elmsheuser⁹⁸, M Elsing³⁰, D Emelianov¹²⁹, R Engelmann¹⁴⁸, A Engl⁹⁸, B Epp⁶¹, J Erdmann¹⁷⁶, A Ereditato¹⁷, D Eriksson^{146a}, J Ernst², M Ernst²⁵, J Ernwein¹³⁶, D Errede¹⁶⁵, S Errede¹⁶⁵, E Ertel⁸¹, M Escalier¹¹⁵, H Esch⁴³, C Escobar¹²³, X Espinal Curull¹², B Esposito⁴⁷, F Etienne⁸³, A I Etievre¹³⁶, E Etzion¹⁵³, D Evangelakou⁵⁴, H Evans⁶⁰, L Fabbri^{20a,20b}, C Fabre³⁰, R M Fakhruddinov¹²⁸, S Falciano^{132a}, Y Fang^{33a}, M Fanti^{89a,89b}, A Farbin⁸, A Farilla^{134a}, J Farley¹⁴⁸, T Farooque¹⁵⁸, S Farrell¹⁶³, S M Farrington¹⁷⁰, P Farthouat³⁰, F Fassi¹⁶⁷, P Fassnacht³⁰, D Fassouliotis⁹, B Fatholahzadeh¹⁵⁸, A Favareto^{89a,89b}, L Fayard¹¹⁵, P Federic^{144a}, O L Fedin¹²¹, W Fedorko¹⁶⁸, M Fehling-Kaschek⁴⁸, L Felgioni⁸³, C Feng^{33d}, E J Feng⁶, A B Fenyuk¹²⁸, J Ferencei^{144b}, W Fernando⁶, S Ferrag⁵³, J Ferrando⁵³, V Ferrara⁴², A Ferrari¹⁶⁶, P Ferrari¹⁰⁵, R Ferrari^{119a}, D E Ferreira de Lima⁵³, A Ferrer¹⁶⁷, D Ferrere⁴⁹, C Ferretti⁸⁷, A Ferretto Parodi^{50a,50b}, M Fiascaris³¹, F Fiedler⁸¹, A Filipčić⁷⁴, F Filthaut¹⁰⁴, M Fincke-Keeler¹⁶⁹, M C N Fiolhais^{124a,187}, L Fiorini¹⁶⁷, A Firan⁴⁰, G Fischer⁴², M J Fisher¹⁰⁹, E A Fitzgerald²³, M Flechl⁴⁸, I Fleck¹⁴¹, P Fleischmann¹⁷⁴, S Fleischmann¹⁷⁵, G T Fletcher¹³⁹, G Fletcher⁷⁵, T Flick¹⁷⁵, A Floderus⁷⁹, L R Flores Castillo¹⁷³, A C Florez Bustos^{159b}, M J Flowerdew⁹⁹, T Fonseca Martin¹⁷, A Formica¹³⁶, A Forti⁸², D Fortin^{159a}, D Fournier¹¹⁵, A J Fowler⁴⁵, H Fox⁷¹, P Francavilla¹², M Franchini^{20a,20b}, S Franchino³⁰, D Francis³⁰, T Frank¹⁷², M Franklin⁵⁷, S Franz³⁰, M Fraternali^{119a,119b}, S Fratina¹²⁰, S T French²⁸, C Friedrich⁴², F Friedrich⁴⁴, D Froidevaux³⁰, J A Frost²⁸, C Fukunaga¹⁵⁶, E Fullana Torregrosa¹²⁷, B G Fulson¹⁴³, J Fuster¹⁶⁷, C Gabaldon³⁰, O Gabizon¹⁷², S Gadatsch¹⁰⁵, T Gadfort²⁵, S Gadomski⁴⁹, G Gagliardi^{50a,50b}, P Gagnon⁶⁰, C Galea⁹⁸, B Galhardo^{124a}, E J Gallas¹¹⁸, V Gallo¹⁷, B J Gallop¹²⁹, P Gallus¹²⁶, K K Gan¹⁰⁹, Y S Gao^{143,185}, A Gaponenko¹⁵, F M Garay Walls⁴⁶, F Garberson¹⁷⁶, M Garcia-Sciveres¹⁵, C García¹⁶⁷, J E García Navarro¹⁶⁷, R W Gardner³¹, N Garelli¹⁴³, V Garonne³⁰, C Gatti⁴⁷, G Gaudio^{119a}, B Gaur¹⁴¹, L Gauthier⁹³, P Gauzzi^{132a,132b}, I L Gavrilenko⁹⁴, C Gay¹⁶⁸, G Gaycken²¹, E N Gazis¹⁰, P Ge^{33d}, Z Gece¹⁶⁸, C N P Gee¹²⁹, D A A Geerts¹⁰⁵, Ch Geich-Gimbel²¹, K Gellerstedt^{146a,146b}, C Gemme^{50a}, A Gemmell⁵³, M H Genest⁵⁵, S Gentile^{132a,132b}, M George⁵⁴, S George⁷⁶, D Gerbaudo¹², P Gerlach¹⁷⁵, A Gershon¹⁵³, C Geweniger^{58a}, H Ghazlane^{135b}, N Ghodbane³⁴, B Giacobbe^{20a}, S Giagu^{132a,132b}, V Giangiobbe¹², F Gianotti³⁰, B Gibbard²⁵, A Gibson¹⁵⁸, S M Gibson³⁰, M Gilchriese¹⁵, T P S Gillam²⁸, D Gillberg³⁰, A R Gillman¹²⁹, D M Gingrich^{3,184}, J Ginzburg¹⁵³, N Giokaris⁹, M P Giordani^{164c}, R Giordano^{102a,102b}, F M Giorgi¹⁶, P Giovannini⁹⁹, P F Giraud¹³⁶, D Giugni^{89a}, M Giunta⁹³, B K Gjelsten¹¹⁷, L K Gladilin⁹⁷, C Glasman⁸⁰, J Glatzer²¹, A Glazov⁴², G L Glonti⁶⁴, J R Goddard⁷⁵, J Godfrey¹⁴², J Godlewski³⁰, M Goebel⁴², T Göpfert⁴⁴, C Goeringer⁸¹, C Gössling⁴³, S Goldfarb⁸⁷, T Golling¹⁷⁶, D Golubkov¹²⁸, A Gomes^{124a,181}, L S Gomez Fajardo⁴², R Gonçalo⁷⁶, J Goncalves Pinto Firmino Da Costa⁴², L Gonella²¹, S González de la Hoz¹⁶⁷, G Gonzalez Parra¹², M L Gonzalez Silva²⁷, S Gonzalez-Sevilla⁴⁹,

J J Goodson¹⁴⁸, L Goossens³⁰, P A Gorbounov⁹⁵, H A Gordon²⁵, I Gorelov¹⁰³, G Gorfine¹⁷⁵, B Gorini³⁰, E Gorini^{72a,72b}, A Gorišek⁷⁴, E Gornicki³⁹, A T Goshaw⁶, M Gosselink¹⁰⁵, M I Gostkin⁶⁴, I Gough Eschrich¹⁶³, M Gouighri^{135a}, D Goujdami^{135c}, M P Goulette⁴⁹, A G Goussiou¹³⁸, C Goy⁵, S Gozpinar²³, I Grabowska-Bold³⁸, P Grafström^{20a,20b}, K-J Grahn⁴², E Gramstad¹¹⁷, F Grancagnolo^{72a}, S Grancagnolo¹⁶, V Grassi¹⁴⁸, V Gratchev¹²¹, H M Gray³⁰, J A Gray¹⁴⁸, E Graziani^{134a}, O G Grebenyuk¹²¹, T Greenshaw⁷³, Z D Greenwood^{25,191}, K Gregersen³⁶, I M Gregor⁴², P Grenier¹⁴³, J Griffiths⁸, N Grigalashvili⁶⁴, A A Grillo¹³⁷, K Grimm⁷¹, S Grinstein¹², Ph Gris³⁴, Y V Grishkevich⁹⁷, J-F Grivaz¹¹⁵, A Grohsjean⁴², E Gross¹⁷², J Grosse-Knetter⁵⁴, J Groth-Jensen¹⁷², K Grybel¹⁴¹, D Guest¹⁷⁶, O Gueta¹⁵³, C Guicheney³⁴, E Guido^{50a,50b}, T Guillemin¹¹⁵, S Guindon⁵⁴, U Gul⁵³, J Gunther¹²⁵, B Guo¹⁵⁸, J Guo³⁵, P Gutierrez¹¹¹, N Guttman¹⁵³, O Gutzwiller¹⁷³, C Guyot¹³⁶, C Gwenlan¹¹⁸, C B Gwilliam⁷³, A Haas¹⁰⁸, S Haas³⁰, C Haber¹⁵, H K Hadavand⁸, D R Hadley¹⁸, P Haefner²¹, Z Hajduk³⁹, H Hakobyan¹⁷⁷, D Hall¹¹⁸, G Halladjian⁶², K Hamacher¹⁷⁵, P Hamal¹¹³, K Hamano⁸⁶, M Hamer⁵⁴, A Hamilton^{145b,193}, S Hamilton¹⁶¹, L Han^{33b}, K Hanagaki¹¹⁶, K Hanawa¹⁶⁰, M Hance¹⁵, C Handel⁸¹, P Hanke^{58a}, J R Hansen³⁶, J B Hansen³⁶, J D Hansen³⁶, P H Hansen³⁶, P Hansson¹⁴³, K Hara¹⁶⁰, T Harenberg¹⁷⁵, S Harkusha⁹⁰, D Harper⁸⁷, R D Harrington⁴⁶, O M Harris¹³⁸, J Hartert⁴⁸, F Hartjes¹⁰⁵, T Haruyama⁶⁵, A Harvey⁵⁶, S Hasegawa¹⁰¹, Y Hasegawa¹⁴⁰, S Hassani¹³⁶, S Haug¹⁷, M Hauschild³⁰, R Hauser⁸⁸, M Havranek²¹, C M Hawkes¹⁸, R J Hawkins³⁰, A D Hawkins⁷⁹, T Hayakawa⁶⁶, T Hayashi¹⁶⁰, D Hayden⁷⁶, C P Hays¹¹⁸, H S Hayward⁷³, S J Haywood¹²⁹, S J Head¹⁸, T Heck⁸¹, V Hedberg⁷⁹, L Heelan⁸, S Heim¹²⁰, B Heinemann¹⁵, S Heisterkamp³⁶, L Helary²², C Heller⁹⁸, M Heller³⁰, S Hellman^{146a,146b}, D Hellmich²¹, C Hensens¹², R C W Henderson⁷¹, M Henke^{58a}, A Henrichs¹⁷⁶, A M Henriques Correia³⁰, S Henrot-Versille¹¹⁵, C Hensel⁵⁴, C M Hernandez⁸, Y Hernández Jiménez¹⁶⁷, R Herrberg¹⁶, G Herten⁴⁸, R Hertenberger⁹⁸, L Hervas³⁰, G G Hesketh⁷⁷, N P Hesse¹⁰⁵, R Hickling⁷⁵, E Higón-Rodríguez¹⁶⁷, J C Hill²⁸, K H Hiller⁴², S Hillert²¹, S J Hillier¹⁸, I Hinchliffe¹⁵, E Hines¹²⁰, M Hirose¹¹⁶, F Hirsch⁴³, D Hirschbuehl¹⁷⁵, J Hobbs¹⁴⁸, N Hod¹⁵³, M C Hodgkinson¹³⁹, P Hodgson¹³⁹, A Hoecker³⁰, M R Hoferkamp¹⁰³, J Hoffman⁴⁰, D Hoffmann⁸³, M Hohlfeld⁸¹, S O Holmgren^{146a}, T Holy¹²⁶, J L Holzbauer⁸⁸, T M Hong¹²⁰, L Hooft van Huysduynen¹⁰⁸, S Horner⁴⁸, J-Y Hostachy⁵⁵, S Hou¹⁵¹, A Houmada^{135a}, J Howard¹¹⁸, J Howarth⁸², M Hrabovsky¹¹³, I Hristova¹⁶, J Hrivnac¹¹⁵, T Hryn'ova⁵, P J Hsu⁸¹, S-C Hsu¹³⁸, D Hu³⁵, Z Hubacek³⁰, F Hubaut⁸³, F Huegging²¹, T A Hülsing⁸¹, A Huettmann⁴², T B Huffman¹¹⁸, E W Hughes³⁵, G Hughes⁷¹, M Huhtinen³⁰, M Hurwitz¹⁵, N Huseynov^{64,194}, J Huston⁸⁸, J Huth⁵⁷, G Iacobucci⁴⁹, G Iakovidis¹⁰, M Ibbotson⁸², I Ibragimov¹⁴¹, L Iconomidou-Fayard¹¹⁵, J Idarraga¹¹⁵, P Iengo^{102a}, O Igonkina¹⁰⁵, Y Ikegami⁶⁵, K Ikematsu¹⁴¹, M Ikeno⁶⁵, D Iliadis¹⁵⁴, N Ilic¹⁵⁸, T Ince⁹⁹, P Ioannou⁹, M Iodice^{134a}, K Iordanidou⁹, V Ippolito^{132a,132b}, A Irls Quiles¹⁶⁷, C Isaksson¹⁶⁶, M Ishino⁶⁷, M Ishitsuka¹⁵⁷, R Ishmukhametov¹⁰⁹, C Issever¹¹⁸, S Istin^{19a}, A V Ivashin¹²⁸, W Iwanski³⁹, H Iwasaki⁶⁵, J M Izen⁴¹, V Izzo^{102a}, B Jackson¹²⁰, J N Jackson⁷³, P Jackson¹, M R Jaekel³⁰, V Jain², K Jakobs⁴⁸, S Jakobsen³⁶, T Jakoubek¹²⁵, J Jakubek¹²⁶, D O Jamin¹⁵¹, D K Jana¹¹¹, E Jansen⁷⁷, H Jansen³⁰, J Janssen²¹, A Jantsch⁹⁹, M Janus⁴⁸, R C Jared¹⁷³, G Jarlskog⁷⁹, L Jeanty⁵⁷, I Jen-La Plante³¹, G-Y Jeng¹⁵⁰, D Jennens⁸⁶, P Jenni³⁰, A E Loevschall-Jensen³⁶, P Jež³⁶, S Jézéquel⁵, M K Jha^{20a}, H Ji¹⁷³, W Ji⁸¹, J Jia¹⁴⁸, Y Jiang^{33b}, M Jimenez Belenguer⁴², S Jin^{33a}, O Jinnouchi¹⁵⁷, M D Joergensen³⁶, D Joffe⁴⁰, M Johansen^{146a,146b}, K E Johansson^{146a}, P Johansson¹³⁹, S Johnert⁴², K A Johns⁷, K Jon-And^{146a,146b}, G Jones¹⁷⁰, R W L Jones⁷¹, T J Jones⁷³, C Joram³⁰, P M Jorge^{124a}, K D Joshi⁸², J Jovicevic¹⁴⁷, T Jovin^{13b}, X Ju¹⁷³, C A Jung⁴³, R M Jungst³⁰, V Juraneck¹²⁵,

P Jussel⁶¹, A Juste Rozas¹², S Kabana¹⁷, M Kaci¹⁶⁷, A Kaczmarzka³⁹, P Kadlecik³⁶, M Kado¹¹⁵, H Kagan¹⁰⁹, M Kagan⁵⁷, E Kajomovitz¹⁵², S Kalinin¹⁷⁵, L V Kalinovskaya⁶⁴, S Kama⁴⁰, N Kanaya¹⁵⁵, M Kaneda³⁰, S Kaneti²⁸, T Kanno¹⁵⁷, V A Kantserov⁹⁶, J Kanzaki⁶⁵, B Kaplan¹⁰⁸, A Kapliy³¹, D Kar⁵³, M Karagounis²¹, K Karakostas¹⁰, M Karnevskiy^{58b}, V Kartvelishvili⁷¹, A N Karyukhin¹²⁸, L Kashif¹⁷³, G Kasieczka^{58b}, R D Kass¹⁰⁹, A Kastanas¹⁴, Y Kataoka¹⁵⁵, J Katzy⁴², V Kaushik⁷, K Kawagoe⁶⁹, T Kawamoto¹⁵⁵, G Kawamura⁸¹, S Kazama¹⁵⁵, V F Kazanin¹⁰⁷, M Y Kazarinov⁶⁴, R Keeler¹⁶⁹, P T Keener¹²⁰, R Kehoe⁴⁰, M Keil⁵⁴, J S Keller¹³⁸, M Kenyon⁵³, H Keoshkerian⁵, O Kepka¹²⁵, N Kerschen³⁰, B P Kerševan⁷⁴, S Kersten¹⁷⁵, K Kessoku¹⁵⁵, J Keung¹⁵⁸, F Khalil-zada¹¹, H Khandanyan^{146a,146b}, A Khanov¹¹², D Kharchenko⁶⁴, A Khodinov⁹⁶, A Khomich^{58a}, T J Khoo²⁸, G Khoriali²¹, A Khoroshilov¹⁷⁵, V Khovanskiy⁹⁵, E Khramov⁶⁴, J Khubua^{51b}, H Kim^{146a,146b}, S H Kim¹⁶⁰, N Kimura¹⁷¹, O Kind¹⁶, B T King⁷³, M King⁶⁶, R S B King¹¹⁸, J Kirk¹²⁹, A E Kiryunin⁹⁹, T Kishimoto⁶⁶, D Kisielewska³⁸, T Kitamura⁶⁶, T Kittelmann¹²³, K Kiuchi¹⁶⁰, E Kladiva^{144b}, M Klein⁷³, U Klein⁷³, K Kleinknecht⁸¹, M Klemetti⁸⁵, A Klier¹⁷², P Klimek^{146a,146b}, A Klimentov²⁵, R Klingenberg⁴³, J A Klinger⁸², E B Klinkby³⁶, T Klioutchnikova³⁰, P F Klok¹⁰⁴, S Klous¹⁰⁵, E-E Kluge^{58a}, T Kluge⁷³, P Kluit¹⁰⁵, S Kluth⁹⁹, E Kneringer⁶¹, E B F G Knoop⁸³, A Knue⁵⁴, B R Ko⁴⁵, T Kobayashi¹⁵⁵, M Kobel⁴⁴, M Kocian¹⁴³, P Kodys¹²⁷, K Köneke³⁰, A C König¹⁰⁴, S Koenig⁸¹, L Köpke⁸¹, F Koetsveld¹⁰⁴, P Koevesarki²¹, T Koffas²⁹, E Koffeman¹⁰⁵, L A Kogan¹¹⁸, S Kohlmann¹⁷⁵, F Kohn⁵⁴, Z Kohout¹²⁶, T Kohriki⁶⁵, T Koi¹⁴³, H Kolanoski¹⁶, V Kolesnikov⁶⁴, I Koletsou^{89a}, J Koll⁸⁸, A A Komar⁹⁴, Y Komori¹⁵⁵, T Kondo⁶⁵, T Kono^{42,195}, A I Kononov⁴⁸, R Konoplich^{108,196}, N Konstantinidis⁷⁷, R Kopeliansky¹⁵², S Koperny³⁸, A K Kopp⁴⁸, K Korcyl³⁹, K Kordas¹⁵⁴, A Korn⁴⁶, A Korol¹⁰⁷, I Korolkov¹², E V Korolkova¹³⁹, V A Korotkov¹²⁸, O Kortner⁹⁹, S Kortner⁹⁹, V V Kostyukhin²¹, S Kotov⁹⁹, V M Kotov⁶⁴, A Kotwal⁴⁵, C Kourkouvelis⁹, V Kouskoura¹⁵⁴, A Koutsman^{159a}, R Kowalewski¹⁶⁹, T Z Kowalski³⁸, W Kozanecki¹³⁶, A S Kozhin¹²⁸, V Kral¹²⁶, V A Kramarenko⁹⁷, G Kramberger⁷⁴, M W Krasny⁷⁸, A Krasznahorkay¹⁰⁸, J K Kraus²¹, F Krauss²¹⁷, A Kravchenko²⁵, S Kreiss¹⁰⁸, F Krejci¹²⁶, J Kretzschmar⁷³, K Kreutzfeldt⁵², N Krieger⁵⁴, P Krieger¹⁵⁸, K Kroeninger⁵⁴, H Kroha⁹⁹, J Kroll¹²⁰, J Kroseberg²¹, J Krstic^{13a}, U Kruchonak⁶⁴, H Krüger²¹, T Kruker¹⁷, N Krumnack⁶³, Z V KrumshTEYN⁶⁴, M K Kruse⁴⁵, T Kubota⁸⁶, S Kuday^{4a}, S Kuehn⁴⁸, A Kugel^{58c}, T Kuhl⁴², V Kukhtin⁶⁴, Y Kulchitsky⁹⁰, S Kuleshov^{32b}, M Kuna⁷⁸, J Kunkle¹²⁰, A Kupco¹²⁵, H Kurashige⁶⁶, M Kurata¹⁶⁰, Y A Kurochkin⁹⁰, V Kus¹²⁵, E S Kuwertz¹⁴⁷, M Kuze¹⁵⁷, J Kvita¹⁴², R Kwee¹⁶, A La Rosa⁴⁹, L La Rotonda^{37a,37b}, L Labarga⁸⁰, S Lablak^{135a}, C Lacasta¹⁶⁷, F Lacava^{132a,132b}, J Lacey²⁹, H Lacker¹⁶, D Lacour⁷⁸, V R Lacuesta¹⁶⁷, E Ladygin⁶⁴, R Lafaye⁵, B Laforge⁷⁸, T Lagouri¹⁷⁶, S Lai⁴⁸, E Laisne⁵⁵, L Lambourne⁷⁷, C L Lampen⁷, W Lampl⁷, E Lancon¹³⁶, U Landgraf⁴⁸, M P J Landon⁷⁵, V S Lang^{58a}, C Lange⁴², A J Lankford¹⁶³, F Lanni²⁵, K Lantzsck³⁰, A Lanza^{119a}, S Laplace⁷⁸, C Lapoire²¹, J F Laporte¹³⁶, T Lari^{89a}, A Larner¹¹⁸, M Lassnig³⁰, P Laurelli⁴⁷, V Lavorini^{37a,37b}, W Lavrijsen¹⁵, P Laycock⁷³, O Le Dortz⁷⁸, E Le Guirriec⁸³, E Le Menedeu¹², T LeCompte⁶, F Ledroit-Guillon⁵⁵, H Lee¹⁰⁵, J S H Lee¹¹⁶, S C Lee¹⁵¹, L Lee¹⁷⁶, M Lefebvre¹⁶⁹, M Legendre¹³⁶, F Legger⁹⁸, C Leggett¹⁵, M Lehmacher²¹, G Lehmann Miotto³⁰, A G Leister¹⁷⁶, M A L Leite^{24d}, R Leitner¹²⁷, D Lellouch¹⁷², B Lemmer⁵⁴, V Lendermann^{58a}, K J C Leney^{145b}, T Lenz¹⁰⁵, G Lenzen¹⁷⁵, B Lenzi³⁰, K Leonhardt⁴⁴, S Leontsinis¹⁰, F Lepold^{58a}, C Leroy⁹³, J-R Lessard¹⁶⁹, C G Lester²⁸, C M Lester¹²⁰, J Levêque⁵, D Levin⁸⁷, L J Levinson¹⁷², A Lewis¹¹⁸, G H Lewis¹⁰⁸, A M Leyko²¹, M Leyton¹⁶, B Li^{33b}, B Li⁸³, H Li¹⁴⁸, H L Li³¹, S Li^{33b,197}, X Li⁸⁷, Z Liang^{118,198}, H Liao³⁴, B Liberti^{133a}, P Lichard³⁰, K Lie¹⁶⁵, W Liebig¹⁴, C Limbach²¹, A Limosani⁸⁶, M Limper⁶², S C Lin^{151,199}, F Linde¹⁰⁵,

J T Linnemann⁸⁸, E Lipeles¹²⁰, A Lipniacka¹⁴, T M Liss¹⁶⁵, D Lissauer²⁵, A Lister⁴⁹, A M Litke¹³⁷, D Liu¹⁵¹, J B Liu^{33b}, L Liu⁸⁷, M Liu^{33b}, Y Liu^{33b}, M Livan^{119a,119b}, S S A Livermore¹¹⁸, A Lleres⁵⁵, J Llorente Merino⁸⁰, S L Lloyd⁷⁵, E Lobodzinska⁴², P Loch⁷, W S Lockman¹³⁷, T Loddenkoetter²¹, F K Loebinger⁸², A Loginov¹⁷⁶, C W Loh¹⁶⁸, T Lohse¹⁶, K Lohwasser⁴⁸, M Lokajicek¹²⁵, V P Lombardo⁵, R E Long⁷¹, L Lopes^{124a}, D Lopez Mateos⁵⁷, J Lorenz⁹⁸, N Lorenzo Martinez¹¹⁵, M Losada¹⁶², P Loscutoff¹⁵, F Lo Sterzo^{132a,132b}, M J Losty^{159a,218}, X Lou⁴¹, A Lounis¹¹⁵, K F Loureiro¹⁶², J Love⁶, P A Love⁷¹, A J Lowe^{143,185}, F Lu^{33a}, H J Lubatti¹³⁸, C Luci^{132a,132b}, A Lucotte⁵⁵, D Ludwig⁴², I Ludwig⁴⁸, J Ludwig⁴⁸, F Luehring⁶⁰, W Lukas⁶¹, L Luminari^{132a}, E Lund¹¹⁷, B Lund-Jensen¹⁴⁷, B Lundberg⁷⁹, J Lundberg^{146a,146b}, O Lundberg^{146a,146b}, J Lundquist³⁶, M Lungwitz⁸¹, D Lynn²⁵, E Lytken⁷⁹, H Ma²⁵, L L Ma¹⁷³, G Maccarrone⁴⁷, A Macchiolo⁹⁹, B Maček⁷⁴, J Machado Miguens^{124a}, D Macina³⁰, R Mackeprang³⁶, R Madar⁴⁸, R J Madaras¹⁵, H J Maddocks⁷¹, W F Mader⁴⁴, A K Madsen¹⁶⁶, M Maeno⁵, T Maeno²⁵, P Mättig¹⁷⁵, S Mättig⁴², L Magnoni¹⁶³, E Magradze⁵⁴, K Mahboubi⁴⁸, J Mahlstedt¹⁰⁵, S Mahmoud⁷³, G Mahout¹⁸, C Maiani¹³⁶, C Maidantchik^{24a}, A Maio^{124a,181}, S Majewski²⁵, Y Makida⁶⁵, N Makovec¹¹⁵, P Mal¹³⁶, B Malaescu⁷⁸, Pa Malecki³⁹, P Malecki³⁹, V P Maleev¹²¹, F Malek⁵⁵, U Mallik⁶², D Malon⁶, C Malone¹⁴³, S Maltezos¹⁰, V Malyshev¹⁰⁷, S Malyukov³⁰, J Mamuzic^{13b}, A Manabe⁶⁵, L Mandelli^{89a}, I Mandić⁷⁴, R Mandrysch⁶², J Maneira^{124a}, A Manfredini⁹⁹, L Manhaes de Andrade Filho^{24b}, J A Manjarres Ramos¹³⁶, A Mann⁹⁸, P M Manning¹³⁷, A Manousakis-Katsikakis⁹, B Mansoulie¹³⁶, R Mantifel⁸⁵, A Mapelli³⁰, L Mapelli³⁰, L March¹⁶⁷, J F Marchand²⁹, F Marchese^{133a,133b}, G Marchiori⁷⁸, M Marcisovsky¹²⁵, C P Marino¹⁶⁹, F Marroquim^{24a}, Z Marshall³⁰, L F Marti¹⁷, S Marti-Garcia¹⁶⁷, B Martin³⁰, B Martin⁸⁸, J P Martin⁹³, T A Martin¹⁸, V J Martin⁴⁶, B Martin dit Latour⁴⁹, S Martin-Haugh¹⁴⁹, H Martinez¹³⁶, M Martinez¹², V Martinez Outschoorn⁵⁷, A C Martyniuk¹⁶⁹, M Marx⁸², F Marzano^{132a}, A Marzin¹¹¹, L Masetti⁸¹, T Mashimo¹⁵⁵, R Mashinistov⁹⁴, J Masik⁸², A L Maslennikov¹⁰⁷, I Massa^{20a,20b}, N Massol⁵, P Mastrandrea¹⁴⁸, A Mastroberardino^{37a,37b}, T Masubuchi¹⁵⁵, H Matsunaga¹⁵⁵, T Matsushita⁶⁶, C Matravers^{118,182}, J Maurer⁸³, S J Maxfield⁷³, D A Maximov^{107,186}, R Mazini¹⁵¹, M Mazur²¹, L Mazzaferro^{133a,133b}, M Mazzanti^{89a}, J Mc Donald⁸⁵, S P Mc Kee⁸⁷, A McCarn¹⁶⁵, R L McCarthy¹⁴⁸, T G McCarthy²⁹, N A McCubbin¹²⁹, K W McFarlane^{56,218}, J A McFayden¹³⁹, G Mchedlidze^{51b}, T McLaughlan¹⁸, S J McMahan¹²⁹, R A McPherson^{169,189}, A Meade⁸⁴, J Mechnich¹⁰⁵, M Mechtel¹⁷⁵, M Medinnis⁴², S Meehan³¹, R Meera-Lebbai¹¹¹, T Meguro¹¹⁶, S Mehlhase³⁶, A Mehta⁷³, K Meier^{58a}, C Meineck⁹⁸, B Meirose⁷⁹, C Melachrinou³¹, B R Mellado Garcia¹⁷³, F Meloni^{89a,89b}, L Mendoza Navas¹⁶², Z Meng^{151,200}, A Mengarelli^{20a,20b}, S Menke⁹⁹, E Meoni¹⁶¹, K M Mercurio⁵⁷, P Mermod⁴⁹, L Merola^{102a,102b}, C Meroni^{89a}, F S Merritt³¹, H Merritt¹⁰⁹, A Messina^{30,201}, J Metcalfe²⁵, A S Mete¹⁶³, C Meyer⁸¹, C Meyer³¹, J-P Meyer¹³⁶, J Meyer³⁰, J Meyer⁵⁴, S Michal³⁰, L Micu^{26a}, R P Middleton¹²⁹, S Migas⁷³, L Mijović¹³⁶, G Mikenberg¹⁷², M Mikestikova¹²⁵, M Mikuž⁷⁴, D W Miller³¹, R J Miller⁸⁸, W J Mills¹⁶⁸, C Mills⁵⁷, A Milov¹⁷², D A Milstead^{146a,146b}, D Milstein¹⁷², G Milutinovic-Dumbelovic^{13a}, A A Minaenko¹²⁸, M Miñano Moya¹⁶⁷, I A Minashvili⁶⁴, A I Mincer¹⁰⁸, B Mindur³⁸, M Mineev⁶⁴, Y Ming¹⁷³, L M Mir¹², G Mirabelli^{132a}, J Mitrevski¹³⁷, V A Mitsou¹⁶⁷, S Mitsui⁶⁵, P S Miyagawa¹³⁹, J U Mjörnmark⁷⁹, T Moa^{146a,146b}, V Moeller²⁸, K Mönig⁴², N Möser²¹, S Mohapatra¹⁴⁸, W Mohr⁴⁸, R Moles-Valls¹⁶⁷, A Molfetas³⁰, J Monk⁷⁷, E Monnier⁸³, J Montejo Berlingen¹², F Monticelli⁷⁰, S Monzani^{20a,20b}, R W Moore³, C Mora Herrera⁴⁹, A Moraes⁵³, N Morange⁶², J Morel⁵⁴, D Moreno⁸¹, M Moreno Llácer¹⁶⁷, P Morettini^{50a}, M Morgenstern⁴⁴, M Morii⁵⁷, A K Morley³⁰, G Mornacchi³⁰, J D Morris⁷⁵,

L Morvaj¹⁰¹, H G Moser⁹⁹, M Mosidze^{51b}, J Moss¹⁰⁹, R Mount¹⁴³, E Mountricha^{10,202}, S V Mouraviev^{94,218}, E J W Moyses⁸⁴, F Mueller^{58a}, J Mueller¹²³, K Mueller²¹, T A Müller⁹⁸, T Mueller⁸¹, D Muenstermann³⁰, Y Munwes¹⁵³, W J Murray¹²⁹, I Mussche¹⁰⁵, E Musto¹⁵², A G Myagkov¹²⁸, M Myska¹²⁵, O Nackenhorst⁵⁴, J Nadal¹², K Nagai¹⁶⁰, R Nagai¹⁵⁷, Y Nagai⁸³, K Nagano⁶⁵, A Nagarkar¹⁰⁹, Y Nagasaka⁵⁹, M Nagel⁹⁹, A M Nairz³⁰, Y Nakahama³⁰, K Nakamura⁶⁵, T Nakamura¹⁵⁵, I Nakano¹¹⁰, H Namasivayam⁴¹, G Nanava²¹, A Napier¹⁶¹, R Narayan^{58b}, M Nash^{77,182}, T Nattermann²¹, T Naumann⁴², G Navarro¹⁶², H A Neal⁸⁷, P Yu Nechaeva⁹⁴, T J Neep⁸², A Negri^{119a,119b}, G Negri³⁰, M Negrini^{20a}, S Nektarijevic⁴⁹, A Nelson¹⁶³, T K Nelson¹⁴³, S Nemecek¹²⁵, P Nemethy¹⁰⁸, A A Nepomuceno^{24a}, M Nessi^{30,203}, M S Neubauer¹⁶⁵, M Neumann¹⁷⁵, A Neusiedl⁸¹, R M Neves¹⁰⁸, P Nevski²⁵, F M Newcomer¹²⁰, P R Newman¹⁸, D H Nguyen⁶, V Nguyen Thi Hong¹³⁶, R B Nickerson¹¹⁸, R Nicolaidou¹³⁶, B Nicquevert³⁰, F Niedercorn¹¹⁵, J Nielsen¹³⁷, N Nikiforou³⁵, A Nikiforov¹⁶, V Nikolaenko¹²⁸, I Nikolic-Audit⁷⁸, K Nikolics⁴⁹, K Nikolopoulos¹⁸, H Nilsen⁴⁸, P Nilsson⁸, Y Ninomiya¹⁵⁵, A Nisati^{132a}, R Nisius⁹⁹, T Nobe¹⁵⁷, L Nodulman⁶, M Nomachi¹¹⁶, I Nomidis¹⁵⁴, S Norberg¹¹¹, M Nordberg³⁰, J Novakova¹²⁷, M Nozaki⁶⁵, L Nozka¹¹³, A-E Nuncio-Quiroz²¹, G Nunes Hanninger⁸⁶, T Nunnemann⁹⁸, E Nurse⁷⁷, B J O'Brien⁴⁶, D C O'Neil¹⁴², V O'Shea⁵³, L B Oakes⁹⁸, F G Oakham^{29,184}, H Oberlack⁹⁹, J Ocariz⁷⁸, A Ochi⁶⁶, S Oda⁶⁹, S Odaka⁶⁵, J Odier⁸³, H Ogren⁶⁰, A Oh⁸², S H Oh⁴⁵, C C Ohm³⁰, T Ohshima¹⁰¹, W Okamura¹¹⁶, H Okawa²⁵, Y Okumura³¹, T Okuyama¹⁵⁵, A Olariu^{26a}, A G Olchevski⁶⁴, S A Olivares Pino⁴⁶, M Oliveira^{124a,187}, D Oliveira Damazio²⁵, E Oliver Garcia¹⁶⁷, D Olivito¹²⁰, A Olszewski³⁹, J Olszowska³⁹, A Onofre^{124a,204}, P U E Onyisi^{31,205}, C J Oram^{159a}, M J Oreglia³¹, Y Oren¹⁵³, D Orestano^{134a,134b}, N Orlando^{72a,72b}, C Oropeza Barrera⁵³, R S Orr¹⁵⁸, B Osculati^{50a,50b}, R Ospanov¹²⁰, C Osuna¹², G Otero y Garzon²⁷, J P Ottersbach¹⁰⁵, M Ouchrif^{135d}, E A Ouellette¹⁶⁹, F Ould-Saada¹¹⁷, A Ouraou¹³⁶, Q Ouyang^{33a}, A Ovcharova¹⁵, M Owen⁸², S Owen¹³⁹, V E Ozcan^{19a}, N Ozturk⁸, A Pacheco Pages¹², C Padilla Aranda¹², S Pagan Griso¹⁵, E Paganis¹³⁹, C Pahl⁹⁹, F Paige²⁵, P Pais⁸⁴, K Pajchel¹¹⁷, G Palacino^{159b}, C P Paleari⁷, S Palestini³⁰, D Pallin³⁴, A Palma^{124a}, J D Palmer¹⁸, Y B Pan¹⁷³, E Panagiotopoulou¹⁰, J G Panduro Vazquez⁷⁶, P Pani¹⁰⁵, N Panikashvili⁸⁷, S Panitkin²⁵, D Pantea^{26a}, A Papadelis^{146a}, Th D Papadopoulou¹⁰, A Paramonov⁶, D Paredes Hernandez³⁴, W Park^{25,206}, M A Parker²⁸, F Parodi^{50a,50b}, J A Parsons³⁵, U Parzefall⁴⁸, S Pashapour⁵⁴, E Pasqualucci^{132a}, S Passaggio^{50a}, A Passeri^{134a}, F Pastore^{134a,134b,218}, Fr Pastore⁷⁶, G Pásztor^{49,207}, S Patarai¹⁷⁵, N D Patel¹⁵⁰, J R Pater⁸², S Patricelli^{102a,102b}, T Pauly³⁰, J Pearce¹⁶⁹, M Pedersen¹¹⁷, S Pedraza Lopez¹⁶⁷, M I Pedraza Morales¹⁷³, S V Peleganchuk¹⁰⁷, D Pelikan¹⁶⁶, H Peng^{33b}, B Penning³¹, A Penson³⁵, J Penwell⁶⁰, T Perez Cavalcanti⁴², E Perez Codina^{159a}, M T Pérez García-Estañ¹⁶⁷, V Perez Reale³⁵, L Perini^{89a,89b}, H Pernegger³⁰, R Perrino^{72a}, P Perrodo⁵, V D Peshekhonov⁶⁴, K Peters³⁰, R F Y Peters⁵⁴, B A Petersen³⁰, J Petersen³⁰, T C Petersen³⁶, E Petit⁵, A Petridis¹⁵⁴, C Petridou¹⁵⁴, E Petrolo^{132a}, F Petrucci^{134a,134b}, D Petschull⁴², M Petteni¹⁴², R Pezoa^{32b}, A Phan⁸⁶, P W Phillips¹²⁹, G Piacquadio³⁰, A Picazio⁴⁹, E Piccaro⁷⁵, M Piccinini^{20a,20b}, S M Piec⁴², R Piegai²⁷, D T Pignotti¹⁰⁹, J E Pilcher³¹, A D Pilkington⁸², J Pina^{124a,181}, M Pinamonti^{164a,164c,208}, A Pinder¹¹⁸, J L Pinfeld³, A Pingel³⁶, B Pinto^{124a}, C Pizio^{89a,89b}, M-A Pleier²⁵, V Pleskot¹²⁷, E Plotnikova⁶⁴, P Plucinski^{146a,146b}, A Poblaguev²⁵, S Poddar^{58a}, F Podlyski³⁴, R Poettgen⁸¹, L Poggioli¹¹⁵, D Pohl²¹, M Pohl⁴⁹, G Polesello^{119a}, A Policicchio^{37a,37b}, R Polifka¹⁵⁸, A Polini^{20a}, J Poll⁷⁵, V Polychronakos²⁵, D Pomeroy²³, K Pommès³⁰, L Pontecorvo^{132a}, B G Pope⁸⁸, G A Popeneciu^{26a}, D S Popovic^{13a}, A Poppleton³⁰, X Portell Bueso³⁰, G E Pospelov⁹⁹, S Pospisil¹²⁶, I N Potrap⁹⁹, C J Potter¹⁴⁹, C T Potter¹¹⁴,

G Poulard³⁰, J Poveda⁶⁰, V Pozdnyakov⁶⁴, R Prabhu⁷⁷, P Pralavorio⁸³, A Pranko¹⁵, S Prasad³⁰, R Pravahan²⁵, S Prell⁶³, K Pretzl¹⁷, D Price⁶⁰, J Price⁷³, L E Price⁶, D Prieur¹²³, M Primavera^{72a}, M Proissl⁴⁶, K Prokofiev¹⁰⁸, F Prokoshin^{32b}, S Protopopescu²⁵, J Proudfoot⁶, X Prudent⁴⁴, M Przybycien³⁸, H Przysieszniak⁵, S Psoroulas²¹, E Ptacek¹¹⁴, E Pueschel⁸⁴, D Puldon¹⁴⁸, M Purohit^{25,206}, P Puzo¹¹⁵, Y Pylypchenko⁶², J Qian⁸⁷, A Quadt⁵⁴, D R Quarrie¹⁵, W B Quayle¹⁷³, M Raas¹⁰⁴, V Radeka²⁵, V Radescu⁴², P Radloff^{ff114}, F Ragusa^{89a,89b}, G Rahal¹⁷⁸, A M Rahimi¹⁰⁹, S Rajagopalan²⁵, M Rammensee⁴⁸, M Rammes¹⁴¹, A S Randle-Conde⁴⁰, K Randrianarivony²⁹, C Rangel-Smith⁷⁸, K Rao¹⁶³, F Rauscher⁹⁸, T C Rave⁴⁸, M Raymond³⁰, A L Read¹¹⁷, D M Rebutti^{119a,119b}, A Redelbach¹⁷⁴, G Redlinger²⁵, R Reece¹²⁰, K Reeves⁴¹, A Reinsch¹¹⁴, I Reisinger⁴³, M Relich¹⁶³, C Rembser³⁰, Z L Ren¹⁵¹, A Renaud¹¹⁵, M Rescigno^{132a}, S Resconi^{89a}, B Resende¹³⁶, P Reznicek⁹⁸, R Rezvani¹⁵⁸, R Richter⁹⁹, E Richter-Was^{5,209}, M Ridel⁷⁸, P Rieck¹⁶, M Rijssenbeek¹⁴⁸, A Rimoldi^{119a,119b}, L Rinaldi^{20a}, R R Rios⁴⁰, E Ritsch⁶¹, I Riu¹², G Rivoltella^{89a,89b}, F Rizatdinova¹¹², E Rizvi⁷⁵, S H Robertson^{85,189}, A Robichaud-Veronneau¹¹⁸, D Robinson²⁸, J E M Robinson⁸², A Robson⁵³, J G Rocha de Lima¹⁰⁶, C Roda^{122a,122b}, D Roda Dos Santos³⁰, A Roe⁵⁴, S Roe³⁰, O Röhne¹¹⁷, S Rolli¹⁶¹, A Romaniouk⁹⁶, M Romano^{20a,20b}, G Romeo²⁷, E Romero Adam¹⁶⁷, N Rompotis¹³⁸, L Roos⁷⁸, E Ros¹⁶⁷, S Rosati^{132a}, K Rosbach⁴⁹, A Rose¹⁴⁹, M Rose⁷⁶, G A Rosenbaum¹⁵⁸, P L Rosendahl¹⁴, O Rosenthal¹⁴¹, L Rossetti⁴⁹, V Rossetti¹², E Rossi^{132a,132b}, L P Rossi^{50a}, M Rotaru^{26a}, I Roth¹⁷², J Rothberg¹³⁸, D Rousseau¹¹⁵, C R Royon¹³⁶, A Rozanov⁸³, Y Rozen¹⁵², X Ruan^{33a,210}, F Rubbo¹², I Rubinskiy⁴², N Ruckstuhl¹⁰⁵, V I Rud⁹⁷, C Rudolph⁴⁴, M S Rudolph¹⁵⁸, F Rühr⁷, A Ruiz-Martinez⁶³, L Romyantsev⁶⁴, Z Rurikova⁴⁸, N A Rusakovich⁶⁴, A Ruschke⁹⁸, J P Rutherford⁷, N Ruthmann⁴⁸, P Ruzicka¹²⁵, Y F Ryabov¹²¹, M Rybar¹²⁷, G Rybkin¹¹⁵, N C Ryder¹¹⁸, A F Saavedra¹⁵⁰, I Sadeh¹⁵³, H F-W Sadrozinski¹³⁷, R Sadykov⁶⁴, F Safai Tehrani^{132a}, H Sakamoto¹⁵⁵, G Salamanna⁷⁵, A Salamon^{133a}, M Saleem¹¹¹, D Salek³⁰, D Salihagic⁹⁹, A Salnikov¹⁴³, J Salt¹⁶⁷, B M Salvachua Ferrando⁶, D Salvatore^{37a,37b}, F Salvatore¹⁴⁹, A Salvucci¹⁰⁴, A Salzburger³⁰, D Sampsonidis¹⁵⁴, A Sanchez^{102a,102b}, V Sanchez Martinez¹⁶⁷, H Sandaker¹⁴, H G Sander⁸¹, M P Sanders⁹⁸, M Sandhoff¹⁷⁵, T Sandoval²⁸, C Sandoval¹⁶², R Sandstroem⁹⁹, D P C Sankey¹²⁹, A Sansoni⁴⁷, C Santamarina Rios⁸⁵, C Santoni³⁴, R Santonico^{133a,133b}, H Santos^{124a}, I Santoyo Castillo¹⁴⁹, K Sapp¹²³, J G Saraiva^{124a}, T Sarangi¹⁷³, E Sarkisyan-Grinbaum⁸, B Sarrazin²¹, F Sarri^{122a,122b}, G Sartisohn¹⁷⁵, O Sasaki⁶⁵, Y Sasaki¹⁵⁵, N Sasao⁶⁷, I Satsounkevitch⁹⁰, G Sauvage^{5,218}, E Sauvan⁵, J B Sauvan¹¹⁵, P Savard^{158,184}, V Savinov¹²³, D O Savu³⁰, L Sawyer^{25,191}, D H Saxon⁵³, J Saxon¹²⁰, C Sbarra^{20a}, A Sbrizzi^{20a,20b}, D A Scannicchio¹⁶³, M Scarcella¹⁵⁰, J Schaarschmidt¹¹⁵, P Schacht⁹⁹, D Schaefer¹²⁰, U Schäfer⁸¹, A Schaelicke⁴⁶, S Schaepe²¹, S Schaezel^{58b}, A C Schaffer¹¹⁵, D Schaile⁹⁸, R D Schamberger¹⁴⁸, V Scharf^{58a}, V A Schegelsky¹²¹, D Scheirich⁸⁷, M Schernau¹⁶³, M I Scherzer³⁵, C Schiavi^{50a,50b}, J Schieck⁹⁸, M Schioppa^{37a,37b}, S Schlenker³⁰, E Schmidt⁴⁸, K Schmieden²¹, C Schmitt⁸¹, C Schmitt⁹⁸, S Schmitt^{58b}, B Schneider¹⁷, Y J Schnellbach⁷³, U Schnoor⁴⁴, L Schoeffel¹³⁶, A Schoening^{58b}, A L S Schorlemmer⁵⁴, M Schott⁸¹, D Schouten^{159a}, J Schovancova¹²⁵, M Schram⁸⁵, C Schroeder⁸¹, N Schroer^{58c}, M J Schultens²¹, J Schultes¹⁷⁵, H-C Schultz-Coulon^{58a}, H Schulz¹⁶, M Schumacher⁴⁸, B A Schumm¹³⁷, Ph Schune¹³⁶, A Schwartzman¹⁴³, Ph Schwegler⁹⁹, Ph Schwemling⁷⁸, R Schvienhorst⁸⁸, J Schwindling¹³⁶, T Schwindt²¹, M Schwoerer⁵, F G Sciacca¹⁷, E Scifo¹¹⁵, G Sciolla²³, W G Scott¹²⁹, J Searcy¹¹⁴, G Sedov⁴², E Sedykh¹²¹, S C Seidel¹⁰³, A Seiden¹³⁷, F Seifert⁴⁴, J M Seixas^{24a}, G Sekhniaidze^{102a}, S J Sekula⁴⁰, K E Selbach⁴⁶, D M Seliverstov¹²¹, B Selliden^{146a}, G Sellers⁷³, M Seman^{144b}, N Semprini-Cesari^{20a,20b}, C Serfon³⁰, L Serin¹¹⁵,

L Serkin⁵⁴, T Serre⁸³, R Seuster^{159a}, H Severini¹¹¹, A Sfyrta³⁰, E Shabalina⁵⁴, M Shamim¹¹⁴, L Y Shan^{33a}, J T Shank²², Q T Shao⁸⁶, M Shapiro¹⁵, P B Shatalov⁹⁵, K Shaw^{164a,164c}, P Sherwood⁷⁷, S Shimizu¹⁰¹, M Shimojima¹⁰⁰, T Shin⁵⁶, M Shiyakova⁶⁴, A Shmeleva⁹⁴, M J Shochet³¹, D Short¹¹⁸, S Shrestha⁶³, E Shulga⁹⁶, M A Shupe⁷, P Sicho¹²⁵, A Sidoti^{132a}, F Siegert⁴⁸, Dj Sijacki^{13a}, O Silbert¹⁷², J Silva^{124a}, Y Silver¹⁵³, D Silverstein¹⁴³, S B Silverstein^{146a}, V Simak¹²⁶, O Simard⁵, Lj Simic^{13a}, S Simion¹¹⁵, E Simioni⁸¹, B Simmons⁷⁷, R Simoniello^{89a,89b}, M Simonyan³⁶, P Sinervo¹⁵⁸, N B Sinev¹¹⁴, V Sipica¹⁴¹, G Siragusa¹⁷⁴, A Sircar²⁵, A N Sisakyan^{64,218}, S Yu Sivoklov⁹⁷, J Sjölin^{146a,146b}, T B Sjusen¹⁴, L A Skinnari¹⁵, H P Skottowe⁵⁷, K Skovpen¹⁰⁷, P Skubic¹¹¹, M Slater¹⁸, T Slavicek¹²⁶, K Sliwa¹⁶¹, V Smakhtin¹⁷², B H Smart⁴⁶, L Smestad¹¹⁷, S Yu Smirnov⁹⁶, Y Smirnov⁹⁶, L N Smirnova^{97,211}, O Smirnova⁷⁹, B C Smith⁵⁷, K M Smith⁵³, M Smizanska⁷¹, K Smolek¹²⁶, A A Snesarev⁹⁴, G Snidero⁷⁵, S W Snow⁸², J Snow¹¹¹, S Snyder²⁵, R Sobie^{169,189}, J Sodomka¹²⁶, A Soffer¹⁵³, C A Solans³⁰, M Solar¹²⁶, J Solc¹²⁶, E Yu Soldatov⁹⁶, U Soldevila¹⁶⁷, E Solfaroli Camillocci^{132a,132b}, A A Solodkov¹²⁸, O V Solovyanov¹²⁸, V Solovyev¹²¹, N Soni¹, A Sood¹⁵, V Sopko¹²⁶, B Sopko¹²⁶, M Sosebee⁸, R Soualah^{164a,164c}, P Soueid⁹³, A Soukharev¹⁰⁷, D South⁴², S Spagnolo^{72a,72b}, F Spanò⁷⁶, R Spighi^{20a}, G Spigo³⁰, R Spiwoks³⁰, M Spousta^{127,212}, T Spreitzer¹⁵⁸, B Spurlock⁸, R D St. Denis⁵³, J Stahlman¹²⁰, R Stamen^{58a}, E Stanecka³⁹, R W Stanek⁶, C Stanescu^{134a}, M Stanescu-Bellu⁴², M M Stanitzki⁴², S Stapnes¹¹⁷, E A Starchenko¹²⁸, J Stark⁵⁵, P Staroba¹²⁵, P Starovoitov⁴², R Staszewski³⁹, A Staude⁹⁸, P Stavina^{144a,218}, G Steele⁵³, P Steinbach⁴⁴, P Steinberg²⁵, I Stekl¹²⁶, B Stelzer¹⁴², H J Stelzer⁸⁸, O Stelzer-Chilton^{159a}, H Stenzel⁵², S Stern⁹⁹, G A Stewart³⁰, J A Stillings²¹, M C Stockton⁸⁵, M Stoebe⁸⁵, K Stoerig⁴⁸, G Stoicea^{26a}, S Stonjek⁹⁹, P Strachota¹²⁷, A R Stradling⁸, A Straessner⁴⁴, J Strandberg¹⁴⁷, S Strandberg^{146a,146b}, A Strandlie¹¹⁷, M Strang¹⁰⁹, E Strauss¹⁴³, M Strauss¹¹¹, P Strizeneč^{144b}, R Ströhmer¹⁷⁴, D M Strom¹¹⁴, J A Strong^{76,218}, R Stroynowski⁴⁰, B Stugu¹⁴, I Stumer^{25,218}, J Stupak¹⁴⁸, P Sturm¹⁷⁵, N A Styles⁴², D A Soh^{151,198}, D Su¹⁴³, H S Subramania³, R Subramaniam²⁵, A Succurro¹², Y Sugaya¹¹⁶, C Suhr¹⁰⁶, M Suk¹²⁷, V V Sulin⁹⁴, S Sultansoy^{4c}, T Sumida⁶⁷, X Sun⁵⁵, J E Sundermann⁴⁸, K Suruliz¹³⁹, G Susinno^{37a,37b}, M R Sutton¹⁴⁹, Y Suzuki⁶⁵, Y Suzuki⁶⁶, M Svatos¹²⁵, S Swedish¹⁶⁸, M Swiatlowski¹⁴³, I Sykora^{144a}, T Sykora¹²⁷, J Sánchez¹⁶⁷, D Ta¹⁰⁵, K Tackmann⁴², A Taffard¹⁶³, R Tafirout^{159a}, N Taiblum¹⁵³, Y Takahashi¹⁰¹, H Takai²⁵, R Takashima⁶⁸, H Takeda⁶⁶, T Takeshita¹⁴⁰, Y Takubo⁶⁵, M Talby⁸³, A Talyshev^{107,186}, J Y C Tam¹⁷⁴, M C Tamsett²⁵, K G Tan⁸⁶, J Tanaka¹⁵⁵, R Tanaka¹¹⁵, S Tanaka¹³¹, S Tanaka⁶⁵, A J Tanasijczuk¹⁴², K Tani⁶⁶, N Tannoury⁸³, S Tapprogge⁸¹, D Tardif¹⁵⁸, S Tarem¹⁵², F Tarrade²⁹, G F Tartarelli^{89a}, P Tas¹²⁷, M Tasevsky¹²⁵, E Tassi^{37a,37b}, Y Tayalati^{135d}, C Taylor⁷⁷, F E Taylor⁹², G N Taylor⁸⁶, W Taylor^{159b}, M Teinturier¹¹⁵, F A Teischinger³⁰, M Teixeira Dias Castanheira⁷⁵, P Teixeira-Dias⁷⁶, K K Temming⁴⁸, H Ten Kate³⁰, P K Teng¹⁵¹, S Terada⁶⁵, K Terashi¹⁵⁵, J Terron⁸⁰, M Testa⁴⁷, R J Teuscher^{158,189}, J Therhaag²¹, T Theveneaux-Pelzer³⁴, S Thoma⁴⁸, J P Thomas¹⁸, E N Thompson³⁵, P D Thompson¹⁸, P D Thompson¹⁵⁸, A S Thompson⁵³, L A Thomsen³⁶, E Thomson¹²⁰, M Thomson²⁸, W M Thong⁸⁶, R P Thun⁸⁷, F Tian³⁵, M J Tibbetts¹⁵, T Tic¹²⁵, V O Tikhomirov⁹⁴, Y A Tikhonov^{107,186}, S Timoshenko⁹⁶, E Tiouchichine⁸³, P Tipton¹⁷⁶, S Tisserant⁸³, T Todorov⁵, S Todorova-Nova¹⁶¹, B Toggerson¹⁶³, J Tojo⁶⁹, S Tokár^{144a}, K Tokushuku⁶⁵, K Tollefson⁸⁸, L Tomlinson⁸², M Tomoto¹⁰¹, L Tompkins³¹, K Toms¹⁰³, A Tonoyan¹⁴, C Topfel¹⁷, N D Topilin⁶⁴, E Torrence¹¹⁴, H Torres⁷⁸, E Torró Pastor¹⁶⁷, J Toth^{83,207}, F Touchard⁸³, D R Tovey¹³⁹, T Trefzger¹⁷⁴, L Tremblet³⁰, A Tricoli³⁰, I M Trigger^{159a}, S Trincaz-Duvoid⁷⁸, M F Tripiana⁷⁰, N Triplett²⁵, W Trischuk¹⁵⁸, B Trocme⁵⁵, C Troncon^{89a}, M Trotter-McDonald¹⁴², M Trovatelli^{134a,134b}, P True⁸⁸,

M Trzebinski³⁹, A Trzupek³⁹, C Tsarouchas³⁰, J C-L Tseng¹¹⁸, M Tsiakiris¹⁰⁵, P V Tsiareshka⁹⁰, D Tsionou^{5,213}, G Tsipolitis¹⁰, S Tsiskaridze¹², V Tsiskaridze⁴⁸, E G Tskhadadze^{51a}, I I Tsukerman⁹⁵, V Tsulaia¹⁵, J-W Tsung²¹, S Tsuno⁶⁵, D Tsybychev¹⁴⁸, A Tua¹³⁹, A Tudorache^{26a}, V Tudorache^{26a}, J M Tuggle³¹, M Turala³⁹, D Turecek¹²⁶, I Turk Cakir^{4d}, R Turra^{89a,89b}, P M Tuts³⁵, A Tykhonov⁷⁴, M Tylmad^{146a,146b}, M Tyndel¹²⁹, G Tzanakos⁹, K Uchida²¹, I Ueda¹⁵⁵, R Ueno²⁹, M Ughetto⁸³, M Ugland¹⁴, M Uhlenbrock²¹, F Ukegawa¹⁶⁰, G Unal³⁰, A Undrus²⁵, G Unel¹⁶³, F C Ungaro⁴⁸, Y Unno⁶⁵, D Urbaniec³⁵, P Urquijo²¹, G Usai⁸, L Vacavant⁸³, V Vacek¹²⁶, B Vachon⁸⁵, S Vahsen¹⁵, N Valencic¹⁰⁵, S Valentinetti^{20a,20b}, A Valero¹⁶⁷, L Valery³⁴, S Valkar¹²⁷, E Valladolid Gallego¹⁶⁷, S Vallecorsa¹⁵², J A Valls Ferrer¹⁶⁷, R Van Berg¹²⁰, P C Van Der Deijl¹⁰⁵, R van der Geer¹⁰⁵, H van der Graaf¹⁰⁵, R Van Der Leeuw¹⁰⁵, E van der Poel¹⁰⁵, D van der Ster³⁰, N van Eldik³⁰, P van Gemmeren⁶, J Van Nieuwkoop¹⁴², I van Vulpen¹⁰⁵, M Vanadia⁹⁹, W Vandelli³⁰, A Vaniachine⁶, P Vankov⁴², F Vannucci⁷⁸, R Vari^{132a}, E W Varnes⁷, T Varol⁸⁴, D Varouchas¹⁵, A Vartapetian⁸, K E Varvell¹⁵⁰, V I Vassilakopoulos⁵⁶, F Vazeille³⁴, T Vazquez Schroeder⁵⁴, F Veloso^{124a}, S Veneziano^{132a}, A Ventura^{72a,72b}, D Ventura⁸⁴, M Venturi⁴⁸, N Venturi¹⁵⁸, V Vercesi^{119a}, M Verducci¹³⁸, W Verkerke¹⁰⁵, J C Vermeulen¹⁰⁵, A Vest⁴⁴, M C Vetterli^{142,184}, I Vichou¹⁶⁵, T Vickey^{145b,214}, O E Vickey Boeriu^{145b}, G H A Viehhauser¹¹⁸, S Viel¹⁶⁸, M Villa^{20a,20b}, M Villaplana Perez¹⁶⁷, E Vilucchi⁴⁷, M G Vincker²⁹, E Vinek³⁰, V B Vinogradov⁶⁴, J Virzi¹⁵, O Vitells¹⁷², M Viti⁴², I Vivarelli⁴⁸, F Vives Vaque³, S Vlachos¹⁰, D Vladioiu⁹⁸, M Vlasak¹²⁶, A Vogel²¹, P Vokac¹²⁶, G Volpi⁴⁷, M Volpi⁸⁶, G Volpini^{89a}, H von der Schmitt⁹⁹, H von Radziewski⁴⁸, E von Toerne²¹, V Vorobel¹²⁷, V Vorwerk¹², M Vos¹⁶⁷, R Voss³⁰, J H Vosseveld⁷³, N Vranjes¹³⁶, M Vranjes Milosavljevic¹⁰⁵, V Vrba¹²⁵, M Vreeswijk¹⁰⁵, T Vu Anh⁴⁸, R Vuillermet³⁰, I Vukotic³¹, Z Vykydal¹²⁶, W Wagner¹⁷⁵, P Wagner²¹, H Wahlen¹⁷⁵, S Wahrmond⁴⁴, J Wakabayashi¹⁰¹, S Walch⁸⁷, J Walder⁷¹, R Walker⁹⁸, W Walkowiak¹⁴¹, R Wall¹⁷⁶, P Waller⁷³, B Walsh¹⁷⁶, C Wang⁴⁵, H Wang¹⁷³, H Wang⁴⁰, J Wang¹⁵¹, J Wang^{33a}, K Wang⁸⁵, R Wang¹⁰³, S M Wang¹⁵¹, T Wang²¹, X Wang¹⁷⁶, A Warburton⁸⁵, C P Ward²⁸, D R Wardrope⁷⁷, M Warsinsky⁴⁸, A Washbrook⁴⁶, C Wasicki⁴², I Watanabe⁶⁶, P M Watkins¹⁸, A T Watson¹⁸, I J Watson¹⁵⁰, M F Watson¹⁸, G Watts¹³⁸, S Watts⁸², A T Waugh¹⁵⁰, B M Waugh⁷⁷, M S Weber¹⁷, J S Webster³¹, A R Weidberg¹¹⁸, P Weigell⁹⁹, J Weingarten⁵⁴, C Weiser⁴⁸, P S Wells³⁰, T Wenaus²⁵, D Wendland¹⁶, Z Weng^{151,198}, T Wengler³⁰, S Wenig³⁰, N Wermes²¹, M Werner⁴⁸, P Werner³⁰, M Werth¹⁶³, M Wessels^{58a}, J Wetter¹⁶¹, C Weydert⁵⁵, K Whalen²⁹, A White⁸, M J White⁸⁶, S White^{122a,122b}, S R Whitehead¹¹⁸, D Whiteson¹⁶³, D Whittington⁶⁰, D Wicke¹⁷⁵, F J Wickens¹²⁹, W Wiedenmann¹⁷³, M Wielers¹²⁹, P Wienemann²¹, C Wiglesworth⁷⁵, L A M Wiik-Fuchs²¹, P A Wijeratne⁷⁷, A Wildauer⁹⁹, M A Wildt^{42,195}, I Wilhelm¹²⁷, H G Wilkens³⁰, J Z Will⁹⁸, E Williams³⁵, H H Williams¹²⁰, S Williams²⁸, W Willis^{35,218}, S Willocq⁸⁴, J A Wilson¹⁸, M G Wilson¹⁴³, A Wilson⁸⁷, I Wingerter-Seez⁵, S Winkelmann⁴⁸, F Winklmeier³⁰, M Wittgen¹⁴³, T Wittig⁴³, J Wittkowski⁹⁸, S J Wollstadt⁸¹, M W Wolter³⁹, H Wolters^{124a,187}, W C Wong⁴¹, G Wooden⁸⁷, B K Wosiek³⁹, J Wotschack³⁰, M J Woudstra⁸², K W Wozniak³⁹, K Wraight⁵³, M Wright⁵³, B Wrona⁷³, S L Wu¹⁷³, X Wu⁴⁹, Y Wu^{33b,215}, E Wulf³⁵, B M Wynne⁴⁶, S Xella³⁶, M Xiao¹³⁶, S Xie⁴⁸, C Xu^{33b}, D Xu^{33a}, L Xu^{33b}, B Yabsley¹⁵⁰, S Yacoob^{145a,216}, M Yamada⁶⁵, H Yamaguchi¹⁵⁵, A Yamamoto⁶⁵, K Yamamoto⁶³, S Yamamoto¹⁵⁵, T Yamamura¹⁵⁵, T Yamanaka¹⁵⁵, K Yamauchi¹⁰¹, T Yamazaki¹⁵⁵, Y Yamazaki⁶⁶, Z Yan²², H Yang^{33e}, H Yang¹⁷³, U K Yang⁸², Y Yang¹⁰⁹, Z Yang^{146a,146b}, S Yanush⁹¹, L Yao^{33a}, Y Yasu⁶⁵, E Yatsenko⁴², J Ye⁴⁰, S Ye²⁵, A L Yen⁵⁷, M Yilmaz^{4b}, R Yoosoofmiya¹²³, K Yorita¹⁷¹, R Yoshida⁶, K Yoshihara¹⁵⁵, C Young¹⁴³,

C J Young¹¹⁸, S Youssef²², D Yu²⁵, D R Yu¹⁵, J Yu⁸, J Yu¹¹², L Yuan⁶⁶, A Yurkewicz¹⁰⁶, B Zabinski³⁹, R Zaidan⁶², A M Zaitsev¹²⁸, S Zambito²³, L Zanello^{132a,132b}, D Zanzi⁹⁹, A Zaytsev²⁵, C Zeitnitz¹⁷⁵, M Zeman¹²⁶, A Zemla³⁹, O Zenin¹²⁸, T Ženiš^{144a}, Z Zinonos^{122a,122b}, D Zerwas¹¹⁵, G Zevi della Porta⁵⁷, D Zhang⁸⁷, H Zhang⁸⁸, J Zhang⁶, L Zhang¹⁵¹, X Zhang^{33d}, Z Zhang¹¹⁵, L Zhao¹⁰⁸, Z Zhao^{33b}, A Zhemchugov⁶⁴, J Zhong¹¹⁸, B Zhou⁸⁷, N Zhou¹⁶³, Y Zhou¹⁵¹, C G Zhu^{33d}, H Zhu⁴², J Zhu⁸⁷, Y Zhu^{33b}, X Zhuang^{33a}, V Zhuravlov⁹⁹, A Zibell⁹⁸, D Zieminska⁶⁰, N I Zimin⁶⁴, R Zimmermann²¹, S Zimmermann²¹, S Zimmermann⁴⁸, M Ziolkowski¹⁴¹, R Zitoun⁵, L Živković³⁵, V V Zmouchko^{128,218}, G Zobernig¹⁷³, A Zoccoli^{20a,20b}, M zur Nedden¹⁶, V Zutshi¹⁰⁶ and L Zwalinski³⁰

¹ School of Chemistry and Physics, University of Adelaide, Adelaide, Australia

² Physics Department, SUNY Albany, Albany, NY, USA

³ Department of Physics, University of Alberta, Edmonton, AB, Canada

^{4a} Department of Physics, Ankara University, Ankara, Turkey

^{4b} Department of Physics, Gazi University, Ankara, Turkey

^{4c} Division of Physics, TOBB University of Economics and Technology, Ankara, Turkey

^{4d} Turkish Atomic Energy Authority, Ankara, Turkey

⁵ LAPP, CNRS/IN2P3 and Université de Savoie, Annecy-le-Vieux, France

⁶ High Energy Physics Division, Argonne National Laboratory, Argonne, IL, USA

⁷ Department of Physics, University of Arizona, Tucson, AZ, USA

⁸ Department of Physics, The University of Texas at Arlington, Arlington, TX, USA

⁹ Physics Department, University of Athens, Athens, Greece

¹⁰ Physics Department, National Technical University of Athens, Zografou, Greece

¹¹ Institute of Physics, Azerbaijan Academy of Sciences, Baku, Azerbaijan

¹² Institut de Física d'Altes Energies and Departament de Física de la Universitat Autònoma de Barcelona and ICREA, Barcelona, Spain

^{13a} Institute of Physics, University of Belgrade, Belgrade, Serbia

^{13b} Vinca Institute of Nuclear Sciences, University of Belgrade, Belgrade, Serbia

¹⁴ Department for Physics and Technology, University of Bergen, Bergen, Norway

¹⁵ Physics Division, Lawrence Berkeley National Laboratory and University of California, Berkeley, CA, USA

¹⁶ Department of Physics, Humboldt University, Berlin, Germany

¹⁷ Albert Einstein Center for Fundamental Physics and Laboratory for High Energy Physics, University of Bern, Bern, Switzerland

¹⁸ School of Physics and Astronomy, University of Birmingham, Birmingham, UK

^{19a} Department of Physics, Bogazici University, Istanbul, Turkey

^{19b} Division of Physics, Dogus University, Istanbul, Turkey

^{19c} Department of Physics Engineering, Gaziantep University, Gaziantep, Turkey

^{19d} Department of Physics, Istanbul Technical University, Istanbul, Turkey

^{20a} INFN Sezione di Bologna, Bologna, Italy

^{20b} Dipartimento di Fisica, Università di Bologna, Bologna, Italy

²¹ Physikalisches Institut, University of Bonn, Bonn, Germany

²² Department of Physics, Boston University, Boston, MA, USA

²³ Department of Physics, Brandeis University, Waltham, MA, USA

^{24a} Universidade Federal do Rio De Janeiro COPPE/EE/IF, Rio de Janeiro, Brazil

^{24b} Federal University of Juiz de Fora (UFJF), Juiz de Fora, Brazil

^{24c} Federal University of Sao Joao del Rei (UFSJ), Sao Joao del Rei, Brazil

- ^{24d} Instituto de Física, Universidade de Sao Paulo, Sao Paulo, Brazil
- ²⁵ Physics Department, Brookhaven National Laboratory, Upton, NY, USA
- ^{26a} National Institute of Physics and Nuclear Engineering, Bucharest, Romania
- ^{26b} University Politehnica Bucharest, Bucharest, Romania
- ^{26c} West University in Timisoara, Timisoara, Romania
- ²⁷ Departamento de Física, Universidad de Buenos Aires, Buenos Aires, Argentina
- ²⁸ Cavendish Laboratory, University of Cambridge, Cambridge, UK
- ²⁹ Department of Physics, Carleton University, Ottawa, ON, Canada
- ³⁰ CERN, Geneva, Switzerland
- ³¹ Enrico Fermi Institute, University of Chicago, Chicago, IL, USA
- ^{32a} Departamento de Física, Pontificia Universidad Católica de Chile, Santiago, Chile
- ^{32b} Departamento de Física, Universidad Técnica Federico Santa María, Valparaíso, Chile
- ^{33a} Institute of High Energy Physics, Chinese Academy of Sciences, Beijing, China
- ^{33b} Department of Modern Physics, University of Science and Technology of China, Anhui, China
- ^{33c} Department of Physics, Nanjing University, Jiangsu, China
- ^{33d} School of Physics, Shandong University, Shandong, China
- ^{33e} Physics Department, Shanghai Jiao Tong University, Shanghai, China
- ³⁴ Laboratoire de Physique Corpusculaire, Clermont Université and Université Blaise Pascal and CNRS/IN2P3, Clermont-Ferrand, France
- ³⁵ Nevis Laboratory, Columbia University, Irvington, NY, USA
- ³⁶ Niels Bohr Institute, University of Copenhagen, Copenhagen, Denmark
- ^{37a} INFN Gruppo Collegato di Cosenza, Università della Calabria, Rende, Italy
- ^{37b} Dipartimento di Fisica, Università della Calabria, Rende, Italy
- ³⁸ AGH University of Science and Technology, Faculty of Physics and Applied Computer Science, Krakow, Poland
- ³⁹ The Henryk Niewodniczanski Institute of Nuclear Physics, Polish Academy of Sciences, Krakow, Poland
- ⁴⁰ Physics Department, Southern Methodist University, Dallas, TX, USA
- ⁴¹ Physics Department, University of Texas at Dallas, Richardson, TX, USA
- ⁴² DESY, Hamburg and Zeuthen, Germany
- ⁴³ Institut für Experimentelle Physik IV, Technische Universität Dortmund, Dortmund, Germany
- ⁴⁴ Institut für Kern- und Teilchenphysik, Technical University Dresden, Dresden, Germany
- ⁴⁵ Department of Physics, Duke University, Durham, NC, USA
- ⁴⁶ SUPA—School of Physics and Astronomy, University of Edinburgh, Edinburgh, UK
- ⁴⁷ INFN Laboratori Nazionali di Frascati, Frascati, Italy
- ⁴⁸ Fakultät für Mathematik und Physik, Albert-Ludwigs-Universität, Freiburg, Germany
- ⁴⁹ Section de Physique, Université de Genève, Geneva, Switzerland
- ^{50a} INFN Sezione di Genova, Università di Genova, Genova, Italy
- ^{50b} Dipartimento di Fisica, Università di Genova, Genova, Italy
- ^{51a} Elepter Andronikashvili Institute of Physics, Ivane Javakhishvili Tbilisi State University, Tbilisi, Georgia
- ^{51b} High Energy Physics Institute, Tbilisi State University, Tbilisi, Georgia
- ⁵² II Physikalisches Institut, Justus-Liebig-Universität Giessen, Giessen, Germany
- ⁵³ SUPA—School of Physics and Astronomy, University of Glasgow, Glasgow, UK

- ⁵⁴ II Physikalisches Institut, Georg-August-Universität, Göttingen, Germany
- ⁵⁵ Laboratoire de Physique Subatomique et de Cosmologie, Université Joseph Fourier and CNRS/IN2P3 and Institut National Polytechnique de Grenoble, Grenoble, France
- ⁵⁶ Department of Physics, Hampton University, Hampton, VA, USA
- ⁵⁷ Laboratory for Particle Physics and Cosmology, Harvard University, Cambridge, MA, USA
- ^{58a} Kirchhoff-Institut für Physik, Ruprecht-Karls-Universität Heidelberg, Heidelberg, Germany
- ^{58b} Physikalisches Institut, Ruprecht-Karls-Universität Heidelberg, Heidelberg, Germany
- ^{58c} ZITI Institut für technische Informatik, Ruprecht-Karls-Universität Heidelberg, Mannheim, Germany
- ⁵⁹ Faculty of Applied Information Science, Hiroshima Institute of Technology, Hiroshima, Japan
- ⁶⁰ Department of Physics, Indiana University, Bloomington, IN, USA
- ⁶¹ Institut für Astro- und Teilchenphysik, Leopold-Franzens-Universität, Innsbruck, Austria
- ⁶² University of Iowa, Iowa City, IA, USA
- ⁶³ Department of Physics and Astronomy, Iowa State University, Ames, IA, USA
- ⁶⁴ Joint Institute for Nuclear Research, JINR Dubna, Dubna, Russia
- ⁶⁵ KEK, High Energy Accelerator Research Organization, Tsukuba, Japan
- ⁶⁶ Graduate School of Science, Kobe University, Kobe, Japan
- ⁶⁷ Faculty of Science, Kyoto University, Kyoto, Japan
- ⁶⁸ Kyoto University of Education, Kyoto, Japan
- ⁶⁹ Department of Physics, Kyushu University, Fukuoka, Japan
- ⁷⁰ Instituto de Física La Plata, Universidad Nacional de La Plata and CONICET, La Plata, Argentina
- ⁷¹ Physics Department, Lancaster University, Lancaster, UK
- ^{72a} INFN Sezione di Lecce, Università del Salento, Lecce, Italy
- ^{72b} Dipartimento di Matematica e Fisica, Università del Salento, Lecce, Italy
- ⁷³ Oliver Lodge Laboratory, University of Liverpool, Liverpool, UK
- ⁷⁴ Department of Physics, Jožef Stefan Institute and University of Ljubljana, Ljubljana, Slovenia
- ⁷⁵ School of Physics and Astronomy, Queen Mary University of London, London, UK
- ⁷⁶ Department of Physics, Royal Holloway University of London, Surrey, UK
- ⁷⁷ Department of Physics and Astronomy, University College London, London, UK
- ⁷⁸ Laboratoire de Physique Nucléaire et de Hautes Energies, UPMC and Université Paris-Diderot and CNRS/IN2P3, Paris, France
- ⁷⁹ Fysiska institutionen, Lunds universitet, Lund, Sweden
- ⁸⁰ Departamento de Física Teórica C-15, Universidad Autónoma de Madrid, Madrid, Spain
- ⁸¹ Institut für Physik, Universität Mainz, Mainz, Germany
- ⁸² School of Physics and Astronomy, University of Manchester, Manchester, UK
- ⁸³ CPPM, Aix-Marseille Université and CNRS/IN2P3, Marseille, France
- ⁸⁴ Department of Physics, University of Massachusetts, Amherst, MA, USA
- ⁸⁵ Department of Physics, McGill University, Montreal, QC, Canada
- ⁸⁶ School of Physics, University of Melbourne, Victoria, Australia
- ⁸⁷ Department of Physics, The University of Michigan, Ann Arbor, MI, USA
- ⁸⁸ Department of Physics and Astronomy, Michigan State University, East Lansing, MI, USA
- ^{89a} INFN Sezione di Milano, Università di Milano, Milano, Italy
- ^{89b} Dipartimento di Fisica, Università di Milano, Milano, Italy
- ⁹⁰ B I Stepanov Institute of Physics, National Academy of Sciences of Belarus, Minsk, Republic of Belarus

- ⁹¹ National Scientific and Educational Centre for Particle and High Energy Physics, Minsk, Republic of Belarus
- ⁹² Department of Physics, Massachusetts Institute of Technology, Cambridge, MA, USA
- ⁹³ Group of Particle Physics, University of Montreal, Montreal, QC, Canada
- ⁹⁴ P N Lebedev Institute of Physics, Academy of Sciences, Moscow, Russia
- ⁹⁵ Institute for Theoretical and Experimental Physics (ITEP), Moscow, Russia
- ⁹⁶ Moscow Engineering and Physics Institute (MEPhI), Moscow, Russia
- ⁹⁷ D V Skobeltsyn Institute of Nuclear Physics, M V Lomonosov Moscow State University, Moscow, Russia
- ⁹⁸ Fakultät für Physik, Ludwig-Maximilians-Universität München, München, Germany
- ⁹⁹ Max-Planck-Institut für Physik (Werner-Heisenberg-Institut), München, Germany
- ¹⁰⁰ Nagasaki Institute of Applied Science, Nagasaki, Japan
- ¹⁰¹ Graduate School of Science and Kobayashi-Maskawa Institute, Nagoya University, Nagoya, Japan
- ^{102a} INFN Sezione di Napoli, Università di Napoli, Napoli, Italy
- ^{102b} Dipartimento di Scienze Fisiche, Università di Napoli, Napoli, Italy
- ¹⁰³ Department of Physics and Astronomy, University of New Mexico, Albuquerque, NM, USA
- ¹⁰⁴ Institute for Mathematics, Astrophysics and Particle Physics, Radboud University Nijmegen/Nikhef, Nijmegen, Netherlands
- ¹⁰⁵ Nikhef National Institute for Subatomic Physics and University of Amsterdam, Amsterdam, Netherlands
- ¹⁰⁶ Department of Physics, Northern Illinois University, DeKalb, IL, USA
- ¹⁰⁷ Budker Institute of Nuclear Physics, SB RAS, Novosibirsk, Russia
- ¹⁰⁸ Department of Physics, New York University, New York, NY, USA
- ¹⁰⁹ Ohio State University, Columbus, OH, USA
- ¹¹⁰ Faculty of Science, Okayama University, Okayama, Japan
- ¹¹¹ Homer L. Dodge Department of Physics and Astronomy, University of Oklahoma, Norman, OK, USA
- ¹¹² Department of Physics, Oklahoma State University, Stillwater, OK, USA
- ¹¹³ Palacký University, RCPTM, Olomouc, Czech Republic
- ¹¹⁴ Center for High Energy Physics, University of Oregon, Eugene, OR, USA
- ¹¹⁵ LAL, Université Paris-Sud and CNRS/IN2P3, Orsay, France
- ¹¹⁶ Graduate School of Science, Osaka University, Osaka, Japan
- ¹¹⁷ Department of Physics, University of Oslo, Oslo, Norway
- ¹¹⁸ Department of Physics, Oxford University, Oxford, UK
- ^{119a} INFN Sezione di Pavia, Pavia, Italy
- ^{119b} Dipartimento di Fisica, Università di Pavia, Pavia, Italy
- ¹²⁰ Department of Physics, University of Pennsylvania, Philadelphia, PA, USA
- ¹²¹ Petersburg Nuclear Physics Institute, Gatchina, Russia
- ^{122a} INFN Sezione di Pisa, Università di Pisa, Pisa, Italy
- ^{122b} Dipartimento di Fisica E. Fermi, Università di Pisa, Pisa, Italy
- ¹²³ Department of Physics and Astronomy, University of Pittsburgh, Pittsburgh, PA, USA
- ^{124a} Laboratório de Instrumentação e Física Experimental de Partículas—LIP, Lisboa, Portugal
- ^{124b} Departamento de Física Teórica y del Cosmos and CAFPE, Universidad de Granada, Granada, Spain
- ¹²⁵ Institute of Physics, Academy of Sciences of the Czech Republic, Praha, Czech Republic

- ¹²⁶ Czech Technical University in Prague, Praha, Czech Republic
- ¹²⁷ Faculty of Mathematics and Physics, Charles University in Prague, Praha, Czech Republic
- ¹²⁸ State Research Center Institute for High Energy Physics, Protvino, Russia
- ¹²⁹ Particle Physics Department, Rutherford Appleton Laboratory, Didcot, UK
- ¹³⁰ Physics Department, University of Regina, Regina, SK, Canada
- ¹³¹ Ritsumeikan University, Kusatsu, Shiga, Japan
- ^{132a} INFN Sezione di Roma I, Università La Sapienza, Roma, Italy
- ^{132b} Dipartimento di Fisica, Università La Sapienza, Roma, Italy
- ^{133a} INFN Sezione di Roma Tor Vergata, Università di Roma Tor Vergata, Roma, Italy
- ^{133b} Dipartimento di Fisica, Università di Roma Tor Vergata, Roma, Italy
- ^{134a} INFN Sezione di Roma Tre, Università Roma Tre, Roma, Italy
- ^{134b} Dipartimento di Fisica, Università Roma Tre, Roma, Italy
- ^{135a} Faculté des Sciences Ain Chock, Réseau Universitaire de Physique des Hautes Energies—Université Hassan II, Casablanca, Morocco
- ^{135b} Centre National de l’Energie des Sciences Techniques Nucleaires, Rabat, Morocco
- ^{135c} Faculté des Sciences Semlalia, Université Cadi Ayyad, LPHEA-Marrakech, Morocco
- ^{135d} Faculté des Sciences, Université Mohamed Premier and LPTPM, Oujda, Morocco
- ^{135e} Faculté des sciences, Université Mohammed V-Agdal, Rabat, Morocco
- ¹³⁶ DSM/IRFU (Institut de Recherches sur les Lois Fondamentales de l’Univers), CEA Saclay (Commissariat à l’Energie Atomique et aux Energies Alternatives), Gif-sur-Yvette, France
- ¹³⁷ Santa Cruz Institute for Particle Physics, University of California Santa Cruz, Santa Cruz, CA, USA
- ¹³⁸ Department of Physics, University of Washington, Seattle, WA, USA
- ¹³⁹ Department of Physics and Astronomy, University of Sheffield, Sheffield, UK
- ¹⁴⁰ Department of Physics, Shinshu University, Nagano, Japan
- ¹⁴¹ Fachbereich Physik, Universität Siegen, Siegen, Germany
- ¹⁴² Department of Physics, Simon Fraser University, Burnaby, BC, Canada
- ¹⁴³ SLAC National Accelerator Laboratory, Stanford, CA, USA
- ^{144a} Faculty of Mathematics, Physics and Informatics, Comenius University, Bratislava, Slovak Republic
- ^{144b} Department of Subnuclear Physics, Institute of Experimental Physics of the Slovak Academy of Sciences, Kosice, Slovak Republic
- ^{145a} Department of Physics, University of Johannesburg, Johannesburg, South Africa
- ^{145b} School of Physics, University of the Witwatersrand, Johannesburg, South Africa
- ^{146a} Department of Physics, Stockholm University, Stockholm, Sweden
- ^{146b} The Oskar Klein Centre, Stockholm, Sweden
- ¹⁴⁷ Physics Department, Royal Institute of Technology, Stockholm, Sweden
- ¹⁴⁸ Departments of Physics and Astronomy and Chemistry, Stony Brook University, Stony Brook, NY, USA
- ¹⁴⁹ Department of Physics and Astronomy, University of Sussex, Brighton, UK
- ¹⁵⁰ School of Physics, University of Sydney, Sydney, Australia
- ¹⁵¹ Institute of Physics, Academia Sinica, Taipei, Taiwan
- ¹⁵² Department of Physics, Technion: Israel Institute of Technology, Haifa, Israel
- ¹⁵³ Raymond and Beverly Sackler School of Physics and Astronomy, Tel Aviv University, Tel Aviv, Israel

- ¹⁵⁴ Department of Physics, Aristotle University of Thessaloniki, Thessaloniki, Greece
- ¹⁵⁵ International Center for Elementary Particle Physics and Department of Physics, The University of Tokyo, Tokyo, Japan
- ¹⁵⁶ Graduate School of Science and Technology, Tokyo Metropolitan University, Tokyo, Japan
- ¹⁵⁷ Department of Physics, Tokyo Institute of Technology, Tokyo, Japan
- ¹⁵⁸ Department of Physics, University of Toronto, Toronto, ON, Canada
- ^{159a} TRIUMF, Vancouver BC, York University, Toronto, ON, Canada
- ^{159b} Department of Physics and Astronomy, York University, Toronto, ON, Canada
- ¹⁶⁰ Faculty of Pure and Applied Sciences, University of Tsukuba, Tsukuba, Japan
- ¹⁶¹ Department of Physics and Astronomy, Tufts University, Medford, MA, USA
- ¹⁶² Centro de Investigaciones, Universidad Antonio Narino, Bogota, Colombia
- ¹⁶³ Department of Physics and Astronomy, University of California Irvine, Irvine, CA, USA
- ^{164a} INFN Gruppo Collegato di Udine, Università di Udine, Udine, Italy
- ^{164b} ICTP, Trieste, Università di Udine, Udine, Italy
- ^{164c} Dipartimento di Chimica, Fisica e Ambiente, Università di Udine, Udine, Italy
- ¹⁶⁵ Department of Physics, University of Illinois, Urbana, IL, USA
- ¹⁶⁶ Department of Physics and Astronomy, University of Uppsala, Uppsala, Sweden
- ¹⁶⁷ Instituto de Física Corpuscular (IFIC) and Departamento de Física Atómica, Molecular y Nuclear and Departamento de Ingeniería Electrónica and Instituto de Microelectrónica de Barcelona (IMB-CNM), University of Valencia and CSIC, Valencia, Spain
- ¹⁶⁸ Department of Physics, University of British Columbia, Vancouver, BC, Canada
- ¹⁶⁹ Department of Physics and Astronomy, University of Victoria, Victoria, BC, Canada
- ¹⁷⁰ Department of Physics, University of Warwick, Coventry, UK
- ¹⁷¹ Waseda University, Tokyo, Japan
- ¹⁷² Department of Particle Physics, The Weizmann Institute of Science, Rehovot, Israel
- ¹⁷³ Department of Physics, University of Wisconsin, Madison, WI, USA
- ¹⁷⁴ Fakultät für Physik und Astronomie, Julius-Maximilians-Universität, Würzburg, Germany
- ¹⁷⁵ Fachbereich C Physik, Bergische Universität Wuppertal, Wuppertal, Germany
- ¹⁷⁶ Department of Physics, Yale University, New Haven, CT, USA
- ¹⁷⁷ Yerevan Physics Institute, Yerevan, Armenia
- ¹⁷⁸ Centre de Calcul de l'Institut National de Physique Nucléaire et de Physique des Particules (IN2P3), Villeurbanne, France
- ¹⁷⁹ Also at Department of Physics, King's College London, London, UK
- ¹⁸⁰ Also at Laboratório de Instrumentação e Física Experimental de Partículas—LIP, Lisboa, Portugal
- ¹⁸¹ Also at Faculdade de Ciências and CFNUL, Universidade de Lisboa, Lisboa, Portugal
- ¹⁸² Also at Particle Physics Department, Rutherford Appleton Laboratory, Didcot, UK
- ¹⁸³ Also at Department of Physics, University of Johannesburg, Johannesburg, South Africa
- ¹⁸⁴ Also at TRIUMF, Vancouver, BC, Canada
- ¹⁸⁵ Also at Department of Physics, California State University, Fresno, CA, USA
- ¹⁸⁶ Also at Novosibirsk State University, Novosibirsk, Russia
- ¹⁸⁷ Also at Department of Physics, University of Coimbra, Coimbra, Portugal
- ¹⁸⁸ Also at Università di Napoli Parthenope, Napoli, Italy
- ¹⁸⁹ Also at Institute of Particle Physics (IPP), Canada
- ¹⁹⁰ Also at Department of Physics, Middle East Technical University, Ankara, Turkey
- ¹⁹¹ Also at Louisiana Tech University, Ruston, LA, USA

¹⁹² Also at Dep Fisica and CEFITEC of Faculdade de Ciencias e Tecnologia, Universidade Nova de Lisboa, Caparica, Portugal

¹⁹³ Also at Department of Physics, University of Cape Town, Cape Town, South Africa

¹⁹⁴ Also at Institute of Physics, Azerbaijan Academy of Sciences, Baku, Azerbaijan

¹⁹⁵ Also at Institut für Experimentalphysik, Universität Hamburg, Hamburg, Germany

¹⁹⁶ Also at Manhattan College, New York, NY, USA

¹⁹⁷ Also at CPPM, Aix-Marseille Université and CNRS/IN2P3, Marseille, France

¹⁹⁸ Also at School of Physics and Engineering, Sun Yat-sen University, Guanzhou, China

¹⁹⁹ Also at Academia Sinica Grid Computing, Institute of Physics, Academia Sinica, Taipei, Taiwan

²⁰⁰ Also at School of Physics, Shandong University, Shandong, China

²⁰¹ Also at Dipartimento di Fisica, Università La Sapienza, Roma, Italy

²⁰² Also at DSM/IRFU (Institut de Recherches sur les Lois Fondamentales de l'Univers), CEA Saclay (Commissariat à l'Énergie Atomique et aux Énergies Alternatives), Gif-sur-Yvette, France

²⁰³ Also at Section de Physique, Université de Genève, Geneva, Switzerland

²⁰⁴ Also at Departamento de Fisica, Universidade de Minho, Braga, Portugal

²⁰⁵ Also at Department of Physics, The University of Texas at Austin, Austin, TX, USA

²⁰⁶ Also at Department of Physics and Astronomy, University of South Carolina, Columbia, SC, USA

²⁰⁷ Also at Institute for Particle and Nuclear Physics, Wigner Research Centre for Physics, Budapest, Hungary

²⁰⁸ Also at International School for Advanced Studies (SISSA), Trieste, Italy

²⁰⁹ Also at Institute of Physics, Jagiellonian University, Krakow, Poland

²¹⁰ Also at LAL, Université Paris-Sud and CNRS/IN2P3, Orsay, France

²¹¹ Also at Faculty of Physics, M V Lomonosov Moscow State University, Moscow, Russia

²¹² Also at Nevis Laboratory, Columbia University, Irvington, NY, USA

²¹³ Also at Department of Physics and Astronomy, University of Sheffield, Sheffield, UK

²¹⁴ Also at Department of Physics, Oxford University, Oxford, UK

²¹⁵ Also at Department of Physics, The University of Michigan, Ann Arbor, MI, USA

²¹⁶ Also at Discipline of Physics, University of KwaZulu-Natal, Durban, South Africa

²¹⁷ Associated author at Durham University, IPPP, Durham, UK

²¹⁸ Deceased

References

- [1] Landshoff P V and Polkinghorne J C 1978 *Phys. Rev. D* **18** 3344
- [2] Takagi F 1979 *Phys. Rev. Lett.* **43** 1296
- [3] Goebel C, Halzen F and Scott D M 1980 *Phys. Rev. D* **22** 2789
- [4] Paver N and Treleani D 1982 *Nuovo Cimento A* **70** 215
- [5] Mekhfi M 1985 *Phys. Rev. D* **32** 2371
- [6] Humpert B 1984 *Phys. Lett. B* **135** 179
- [7] Humpert B and Odorico R 1985 *Phys. Lett. B* **154** 211
- [8] Ametller L, Paver N and Treleani D 1986 *Phys. Lett. B* **169** 289
- [9] Halzen F, Hoyer P and Stirling W J 1987 *Phys. Lett. B* **188** 375–8
- [10] Godbole R M, Gupta S and Lindfors J 1990 *Z. Phys. C* **47** 69–74
- [11] Mekhfi M 1985 *Phys. Rev. D* **32** 2380

- [12] Shelest V P, Snigirev A M and Zinovev G M 1982 *Phys. Lett. B* **113** 325
- [13] ATLAS Collaboration 2011 *Nature Commun.* **2** 463
- [14] Antchev G *et al* (TOTEM Collaboration) 2011 arXiv:1110.1395 [hep-ex]
- [15] Akesson T *et al* (AFS Collaboration) 1987 *Z. Phys. C* **34** 163
- [16] Alitti J *et al* (UA2 Collaboration) 1991 *Phys. Lett. B* **268** 145–54
- [17] Abe F *et al* (CDF Collaboration) 1993 *Phys. Rev. D* **47** 4857–71
- [18] Abe F *et al* (CDF Collaboration) 1997 *Phys. Rev. D* **56** 3811–32
- [19] Abazov V *et al* (D0 Collaboration) 2010 *Phys. Rev. D* **81** 052012
- [20] Calucci G and Treleani D 1999 *Nucl. Phys. Proc. Suppl.* **71** 392–9
- [21] Calucci G and Treleani D 1999 *Phys. Rev. D* **60** 054023
- [22] Ryskin M G and Snigirev A M 2011 *Phys. Rev. D* **83** 114047
- [23] Kom C H, Kulesza A and Stirling W J 2011 arXiv:1109.0309 [hep-ph]
- [24] Gaunt J R and Stirling W J 2010 *J. High Energy Phys.* **JHEP03(2010)005**
- [25] Diehl M and Schafer A 2011 *Phys. Lett. B* **698** 389–402
- [26] Drees M and Han T 1996 *Phys. Rev. Lett.* **77** 4142–5
- [27] Del Fabbro A and Treleani D 2000 *Phys. Rev. D* **61** 077502
- [28] Kulesza A and Stirling W J 2000 *Phys. Lett. B* **475** 168–75
- [29] Del Fabbro A and Treleani D 2002 *Phys. Rev. D* **66** 074012
- [30] Hussein M Y 2007 *Nucl. Phys. Proc. Suppl.* **174** 55–8
- [31] Maina E 2009 *J. High Energy Phys.* **JHEP04(2009)098**
- [32] Maina E 2009 *J. High Energy Phys.* **JHEP09(2009)081**
- [33] Berger E L, Jackson C B and Shaughnessy G 2010 *Phys. Rev. D* **81** 014014
- [34] Gaunt J R *et al* 2010 *Eur. Phys. J. C* **69** 53–65
- [35] Maina E 2011 *J. High Energy Phys.* **JHEP01(2011)061**
- [36] ATLAS Collaboration 2008 *J. Instrum.* **3** S08003
- [37] Blok B *et al* 2012 *Eur. Phys. J. C* **72** 1963
- [38] Blok B *et al* 2011 *Phys. Rev. D* **83** 071501
- [39] Gaunt J R *et al* 2011 arXiv:1110.1174v1 [hep-ex]
- [40] Gaunt J R and Stirling W J 2012 arXiv:1202.3056v1 [hep-ex]
- [41] ATLAS Collaboration 2012 *Phys. Rev. D* **85** 092002
- [42] ATLAS Collaboration 2012 *Eur. Phys. J. C* **72** 1909
- [43] ATLAS Collaboration cds.cern.ch/record/1281339/files/ATLAS-CONF-2010-064.pdf
- [44] Cacciari M, Salam G P and Soyez G 2008 *J. High Energy Phys.* **JHEP04(2008)063**
- [45] ATLAS Collaboration 2005 *Nucl. Instrum. Methods Phys. Res. A* **545** 803
- [46] ATLAS Collaboration CERN-PH-EP-2011-191
- [47] Agostinelli S *et al* 2003 *Nucl. Instrum. Methods Phys. Res. A* **506** 250
- [48] ATLAS Collaboration 2010 *Eur. Phys. J. C* **70** 823
- [49] Pumplin J *et al* 2002 *J. High Energy Phys.* **JHEP07(2002)012**
- [50] Mangano M L *et al* 2003 *J. High Energy Phys.* **JHEP07(2003)001**
- [51] Alwall J *et al* 2008 *Eur. Phys. J. C* **53** 473
- [52] Corcella G *et al* 2001 *J. High Energy Phys.* **JHEP01(2001)010**
- [53] Butterworth J M, Forshaw J R and Seymour M H 1996 *Z. Phys. C* **72** 637–46
- [54] Gleisberg T *et al* 2009 *J. High Energy Phys.* **JHEP02(2009)007**
- [55] Catani S *et al* 2001 *J. High Energy Phys.* **JHEP11(2001)063**
- [56] Sjostrand T, Mrenna S and Skands P Z 2006 *J. High Energy Phys.* **JHEP05(2006)026**
- [57] Alioli S *et al* 2010 *J. High Energy Phys.* **JHEP06(2010)043**
- [58] Frixione S and Webber B R 2002 *J. High Energy Phys.* **JHEP06(2002)029**
- [59] Adye T 2011 arXiv:1105.1160 [hep-ex]